Origin, speciation, and fluxes of trace-element gases at Augustine volcano, Alaska: Insights into magma degassing and fumarolic processes

ROBERT B. SYMONDS,[1,]* MARK H. REED,[2] and WILLIAM I. ROSE[1]

[1]Department of Geological Engineering, Geology and Geophysics, Michigan Technological University, Houghton, MI 49931, USA
[2]Department of Geological Sciences, University of Oregon, Eugene, OR 97403, USA

Abstract—Thermochemical modeling predicts that trace elements in the Augustine gas are transported from near-surface magma as simple chloride ($NaCl$, KCl, $FeCl_2$, $ZnCl_2$, $PbCl_2$, $CuCl$, $SbCl_3$, $LiCl$, $MnCl_2$, $NiCl_2$, $BiCl$, $SrCl_2$), oxychloride (MoO_2Cl_2), sulfide (AsS), and elemental (Cd) gas species. However, Si, Ca, Al, Mg, Ti, V, and Cr are actually more concentrated in solids, beta-quartz (SiO_2), wollastonite ($CaSiO_3$), anorthite ($CaAl_2Si_2O_8$), diopside ($CaMgSi_2O_6$), sphene ($CaTiSiO_5$), $V_2O_3(c)$, and $Cr_2O_3(c)$, respectively, than in their most abundant gaseous species, SiF_4, $CaCl_2$, AlF_2O, $MgCl_2$, $TiCl_4$, $VOCl_3$, and CrO_2Cl_2. These computed solids are not degassing products, but reflect contaminants in our gas condensates or possible problems with our modeling due to "missing" gas species in the thermochemical data base.

Using the calculated distribution of gas species and the COSPEC SO_2 fluxes, we have estimated the emission rates for many species (e.g., COS, NaCl, KCl, HBr, AsS, CuCl). Such forecasts could be useful to evaluate the effects of these trace species on atmospheric chemistry.

Because of the high volatility of metal chlorides (e.g., $FeCl_2$, $NaCl$, KCl, $MnCl_2$, $CuCl$), the extremely HCl-rich Augustine volcanic gases are favorable for transporting metals from magma. Thermochemical modeling shows that equilibrium degassing of magma near 870°C can account for the concentrations of Fe, Na, K, Mn, Cu, Ni, and part of the Mg in the gases escaping from the dome fumaroles on the 1986 lava dome. These calculations also explain why gases escaping from the lower temperature but highly oxidized moat vents on the 1976 lava dome should transport less Fe, Na, K, Mn, and Ni, but more Cu; oxidation may also account for the larger concentrations of Zn and Mo in the moat gases.

Nonvolatile elements (e.g., Al, Ca, Ti, Si) in the gas condensates came from eroded rock particles that dissolved in our samples or, for Si, from contamination from the silica sampling tube. Only a very small amount of rock contamination occurred (water/rock ratios between 10^4 and 10^6). Erosion is more prevalent in the pyroclastic flow fumaroles than in the summit vents, reflecting physical differences in the fumarole walls: ash vs. lava. Trace element contents of volcanic gases show enormous variability because of differences in the intensive parameters of degassing magma and variable amounts of wall rock erosion in volcanic fumaroles.

INTRODUCTION

EXTENSIVE SAMPLING of volcanic fumaroles over the past 70 years has shown that volcanic gases are dominated by six elements, C, O, H, S, Cl, and F which combine to form a few major gas species, H_2O, CO_2, SO_2, H_2S, H_2, HCl, CO, and HF (JAGGER, 1940; GERLACH, 1980a; GERLACH and CASADEVALL, 1986b). Volcanic gases also contain a myriad of trace components such as Br, Na, Mo, Cu, As, and Se, and their respective species (e.g., HBr, NaCl, H_2MoO_4, CuCl, AsS, H_2Se; e.g., SYMONDS et al., 1987; QUISEFIT et al., 1989). Study of trace elements in volcanic gases can provide insight on (1) the molecular form of magmatic fluids (e.g., NAUGHTON et al., 1974; SYMONDS et al., 1987; QUISEFIT et al., 1989; BERNARD et al., 1990), (2) the role of magmatic volatiles in ore deposits (e.g., SYMONDS et al., 1987), and (3) the impact of volcanic emissions on atmospheric chemistry (e.g., BUAT-MÉNARD and ARNOLD, 1978; VAREKAMP and BUSECK, 1986; PATTERSON and SETTLE, 1987). Unfortunately, progress on

the above has been hampered because the origin of trace elements in volcanic gas samples is complex; in addition to magma degassing, they may also be contaminants from the wall rock or sampling equipment (STOIBER and ROSE, 1970; GEMMELL, 1987; QUISEFIT et al., 1989; SYMONDS et al., 1990).

The primary purpose of this work is to determine the origin of trace elements (mostly metals) in condensates (brackish to saline waters collected by condensing volcanic gases) collected by SYMONDS et al. (1990) in 1986–1987 from Augustine volcano, Alaska. We study condensates from Augustine volcano because a wide variety of fumaroles were sampled; these data enable us to study trace element transport in a large array of chemical and physical environments. Specifically, we seek to understand why (1) the highest concentrations of many volatile elements (B, K, Na, Fe, As, Pb, Sb, Cd, Mn, Li, Ni) generally occur in condensates from the high-temperature dome fumarole that vents through 1986 lava; (2) high concentrations of refractory elements (Al, Ca, Mg, Zr, Ba, Sr, Cr) are normally found in samples from the pyroclastic flow fumaroles, which are low-temperature and rootless; and (3) the highest concentrations of Zn, Cu, Mo,

V, and Ti usually occur in the condensates collected from the moderate-temperature, oxidized moat fumaroles on the 1976 dome (Fig. 1).

To determine the origin of trace elements in the Augustine gas condensates, we consider five possible sources:

1) Volatilization from magma (NAUGHTON et al., 1974; SYMONDS et al., 1987). As the major gases exsolve from the magma, forming bubbles, they react with it, volatilizing trace element species (process 1, Fig. 2).

2) Erosion of rock particles from fumarole walls (VIE LE SAGE, 1983; QUISEFIT et al., 1988). Variable amounts of ash, fragments of lava, sublimates, or altered rock may have broken off the vent walls, become entrained in the gas stream, and dissolved in the condensates (process 2, Fig. 2).

3) Mixing of magmatic gases with boiled meteoric water. Meteoric water, enriched with anions from condensed volcanic gases, may be percolating through the wall rock and dissolving andesite. If such solutions seep into fumaroles and boil, they could release gases and aerosols into the gas stream (process 3, Fig. 2).

4) Reaction of condensed acidic species (e.g., sulfuric acid) with the walls of fumaroles and re-entrainment of such reacted liquids into the gas stream (STOIBER and ROSE, 1970) (process 4, Fig. 2).

5) Contamination of Si from the silica tubes used for condensate sampling (TOUTAIN et al., 1990).

The second purpose of this work is to study the molecular form of trace elements that escaped from the Augustine magma using a thermodynamic modeling approach. Because most trace elements in volcanic gases are volatilized as chlorides (SYMONDS et al., 1987) and the Augustine gases are

extremely HCl-rich (SYMONDS et al., 1990), Augustine offers an excellent opportunity to study the transport of metallic and non-metallic elements in Cl-rich gases.

A third purpose of this work is to estimate fluxes of many gas species from Augustine. It is important to estimate the natural volcanic fluxes of (1) greenhouse gases (e.g., CO_2, CH_4) that may cause global warming (GERLACH, 1989); (2) halogen gases (e.g., HCl, HF, HBr) that may destroy ozone in the stratosphere (JOHNSTON, 1980; SYMONDS et al., 1988); (3) acid aerosols (e.g., H_2SO_4) that block incoming solar radiation and thus may effect climate (DEVINE et al., 1984); and (4) toxic metals and their species (BUAT-MÉNARD and ARNOLD, 1978; VAREKAMP and BUSECK, 1986; PATTERSON and SETTLE, 1987). Previous studies have estimated volcanic fluxes of a few major gas species (e.g., CASADEVALL et al., 1983, GREENLAND et al., 1985; ROSE et al., 1986) and trace elements but not their species (e.g., BUAT-MÉNARD and ARNOLD, 1978; PHELAN et al., 1982; VAREKAMP and BUSECK, 1986; PATTERSON and SETTLE, 1987). This study is a first attempt to estimate emission rates for many gas species.

AUGUSTINE VOLCANO AND THE 1986–1987 FUMAROLES

Mount St. Augustine is located on Augustine Island in the Lower Cook Inlet on the eastern Aleutian Arc. It is an andesitic-dacitic volcano, consisting of a central dome complex surrounded by an apron of volcanoclastic deposits (SWANSON and KIENLE, 1988). Augustine is one of the most active Alaskan volcanoes, erupting six times in the past two hundred years (1812, 1883, 1935, 1963–64, 1976, 1986). The 1986 eruptions commenced with explosive activity with numerous pyroclastic flows in late March and early April (SWANSON and KIENLE, 1988). In late April, high-silica andesitic lava was extruded at the base of the 1976 dome, forming a new dome and a short blocky lava flow (SWANSON and KIENLE, 1988). Elevated dome-building activity occurred in late August 1986.
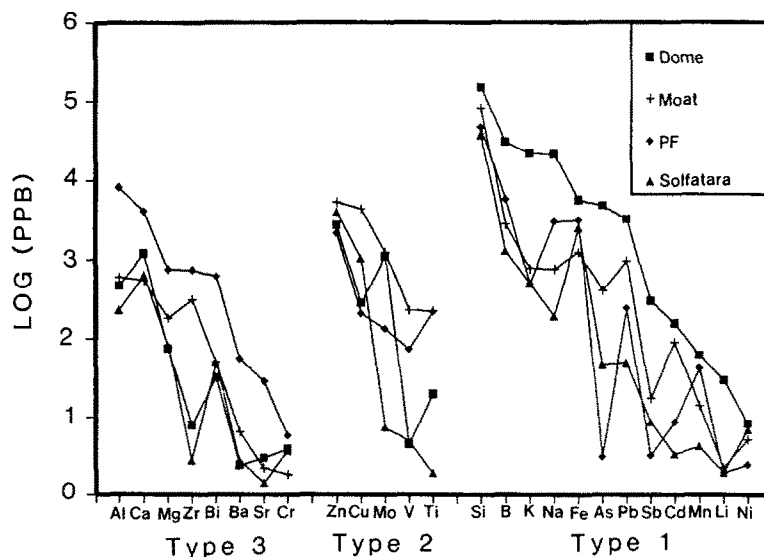
FIG. 1. Geometric mean concentrations of elements in gas condensates collected in 1986–1987 from the dome, moat, solfatara, and pyroclastic flow fumarole fields at Augustine volcano. Elements are subdivided into three groups: Type 1 elements are most abundant in the dome condensates; Type 2 elements are most plentiful in the moat samples; and Type 3 elements have the highest concentrations in the pyroclastic flow specimens. All the samples from each fumarole field were used to calculate the mean; when data were below detection, we used a number midway between the detection limit and zero. Data are from SYMONDS et al. (1990). The geometric deviations are generally less than ±0.5 log ppb units.
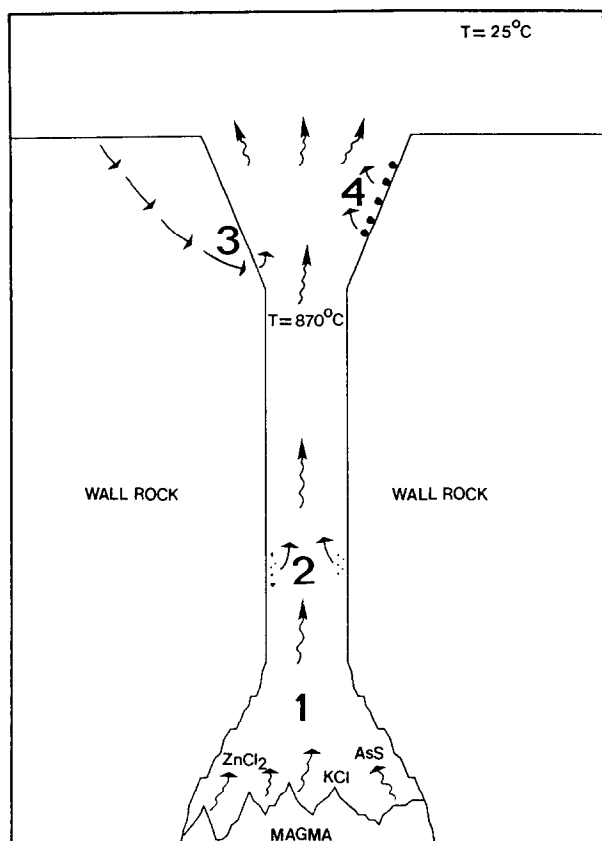
FIG. 2. Schematic diagram showing the possible origins of trace elements transported in the Augustine gases as depicted for the dome fumarole. We have considered four natural sources: (1) release of volatile compounds from magma; (2) erosion of rock particles from the vent walls; (3) boiling of water into the gas that has leached the surrounding andesite; and (4) contamination of volcanic gas by condensed acid liquids that dissolved trace elements from the wall rock.

The fumarole fields sampled by SYMONDS et al. (1990) in the summers of 1986 and 1987, during times of passive degassing, were named the dome, moat, solfatara, and pyroclastic flow sites. The gas and condensate data of SYMONDS et al. (1990) are summarized in Table 1 and Fig. 1.

The dome site is a fumarole field at the base of the spine on the 1986 lava dome. During 1987, one 870°C vent was sampled here. Two restored gas analyses from this vent are shown in Table 1. These gases are mixtures of seawater and magmatic volatiles, but most closely represent the juvenile gases escaping from the Augustine magma reservoir (SYMONDS et al., 1990). The dome condensates generally have the largest concentrations of the group of elements called Type 1 in Fig. 1.

In 1986, the moat vents ranged from 390 to 642°C and issued from concentric cracks on a tephra-covered ramp, the remains of the 1976 lava dome, between the outer crater wall and the inner crater. Two unrestored gas analyses from the moat-1 and moat-4 sites are shown in Table 1. The moat gases are apparently variable mixtures of seawater, magmatic volatiles, and meteoric water (SYMONDS et al., 1990). In contrast to those that emanated from the dome, these gases vented from the more degassed 1976 magma and were more contaminated with meteoric steam and air (SYMONDS et al., 1990). The moat gases have relatively large concentrations of the group of elements labeled Type 2 in Fig. 1.

The solfatara fumarole field is located just outside the summit crater and extends from the margin of the 1964 lava dome to the saddle between the 1964 and 1935 domes. Fumarolic clay mantles the surface of this field. In 1986, gases emanating from the 230 to

318°C solfatara sites had a diluted seawater-magmatic component (SYMONDS et al., 1990) and generally very low concentrations of trace elements (Fig. 1).

After the spring 1986 eruption, there were numerous rootless fumaroles on the cooling pyroclastic flows of which three, 202 to 247°C vents were sampled. They escaped through ash and pumice rather than dense lava, which formed the walls of the summit vents. These gases are mixtures of volatiles escaping from degassed pyroclastic material and meteoric steam (SYMONDS et al., 1990). The pyroclastic flow condensates typically have large concentrations of Type 3 elements (Fig. 1); except for Bi, these are rock-forming elements (SYMONDS et al., 1990).

WORKING HYPOTHESIS

The following calculations are based of the premise that the high-temperature gases that escaped from the dome and moat fumaroles in 1986 and 1987, including any seawater component, were once in contact with magma. For the ensuing modeling, the term magma is used loosely to refer to any hot (>600°C) andesitic-dacitic material, molten or solidified. On the way to the surface, these gases may have mixed with meteoric steam, entrained rock particles, reacted with the wall rock, or mixed with air. Consequently, we presume that the trace elements in the gas are derived from volatilization of magma or from interactions with the wall rock. We base our model on four lines of evidence: (1) the high temperatures (600°-870°C) of the dome and moat fumaroles are consistent with a largely magmatic source or, at least, with the gases being in contact with the magma during the volatilization process; (2) the Augustine summit is 1200 m above sea level so we think it likely that any seawater would have been in contact with magma before discharging from the hot summit vents; (3) H and O isotope data from fumarolic condensates suggest that the dome and moat gases have a magmatic component; evidence that some fraction of the gases issued from magma (SYMONDS et al., 1990); and (4) Mg enrichment factors are consistent with volatile elements coming from magma degassing and refractory elements coming from the wall rock (SYMONDS et al., 1990).

THERMOCHEMICAL MODELING APPROACH

The two restored Augustine dome gas analyses provide information on the major gas species, while the condensate data furnish estimates of the concentration of trace components (e.g., Na, K, Pb, Cu) in the volcanic gas. Thermochemical modeling can indicate whether trace elements in the Augustine gases are direct magma degassing products or come from some other source. In addition, the modeling can (1) allow us to estimate probable trace species (e.g., COS, CS_2, halocarbons) in the H-C-O-S-Cl-F system; (2) predict the molecular form of volatile trace components (e.g., Na, K, Bi) as they leave the magma; (3) help estimate fluxes of many gas species by furnishing ratios of those species to SO_2, whose emission rate can be measured directly by correlation spectrometry (CASADEVALL et al., 1983); and (4) provide a geochemical framework to explain the compositional variations of Augustine's condensates (Fig. 1).

Method of Calculation

Gas calculations were done with SOLVGAS and GAS-WORKS, computer codes for calculating homogeneous and

Table 1.   Reconstructed Augustine gas compositions.
            Modified from Symonds et al. (1990).

Sample	dome-2	dome-3	moat-1	moat-4
Date:	8-28-87	8-28-87	7-9-86	7-9-86
T ($^{\circ}$C):	870	870	431	642
log (fO_2)	-12.45	-12.59	---	---

Major Gas Species (mole fraction)

	dome-2	dome-3	moat-1	moat-4
H_2O	0.8477	0.8391	0.9199	0.9742
HCl	0.0534	0.0604	0.0641	0.0141
SO_2	0.0618	0.0572	0.0034	0.0052
CO_2	0.0227	0.0240	0.00040	0.00029
H_2S	0.0068	0.0100	---	---
H_2	0.0054	0.0063	---	---
S_2	0.0012	0.0020	---	---
HF	0.00086	0.00086	0.0122	0.0062
CO	0.00016	0.00020	---	---
restored[a]	yes	yes	no	no

Trace Elements (mole fraction)

	dome-2	dome-3	moat-1	moat-4
Si	8.4×10^{-5}	8.3×10^{-5}	4.6×10^{-5}	3.0×10^{-5}
B	4.6×10^{-5}	4.5×10^{-5}	1.3×10^{-5}	2.8×10^{-6}
Na	1.5×10^{-5}	1.4×10^{-5}	4.1×10^{-7}	7.7×10^{-7}
K	8.8×10^{-6}	8.7×10^{-6}	---	3.4×10^{-7}
Br	6.9×10^{-6}	6.8×10^{-6}	7.9×10^{-6}	5.5×10^{-6}
Fe	1.6×10^{-6}	1.6×10^{-6}	2.0×10^{-7}	2.7×10^{-7}
As	1.0×10^{-6}	9.9×10^{-7}	1.9×10^{-8}	1.3×10^{-7}
Zn	6.5×10^{-7}	6.4×10^{-7}	5.2×10^{-6}	5.3×10^{-7}
Ca	4.7×10^{-7}	4.6×10^{-7}	2.3×10^{-7}	2.2×10^{-7}
Al	2.7×10^{-7}	2.7×10^{-7}	4.5×10^{-7}	3.6×10^{-7}
Pb	2.4×10^{-7}	2.4×10^{-7}	6.3×10^{-8}	3.7×10^{-8}
Mo	1.8×10^{-7}	1.8×10^{-7}	1.9×10^{-7}	2.3×10^{-7}
Cu	7.0×10^{-8}	6.9×10^{-8}	7.1×10^{-6}	3.3×10^{-7}
Li	6.8×10^{-8}	6.7×10^{-8}	---	---
Mg	4.8×10^{-8}	4.8×10^{-8}	1.1×10^{-7}	9.5×10^{-8}
Sb	3.9×10^{-8}	3.8×10^{-8}	9.0×10^{-10}	1.7×10^{-9}
Cd	2.2×10^{-8}	2.1×10^{-8}	1.7×10^{-8}	9.5×10^{-9}
Mn	1.8×10^{-8}	1.7×10^{-8}	7.0×10^{-9}	5.6×10^{-9}
Ti	6.5×10^{-9}	6.5×10^{-9}	8.1×10^{-8}	3.2×10^{-8}
Bi	2.4×10^{-9}	2.4×10^{-9}	---	---
Ni	2.3×10^{-9}	2.2×10^{-9}	2.9×10^{-9}	---
Zr	1.7×10^{-9}	1.7×10^{-9}	3.0×10^{-8}	1.3×10^{-7}
V	1.5×10^{-9}	1.5×10^{-9}	8.1×10^{-8}	6.4×10^{-8}
Cr	1.2×10^{-9}	1.2×10^{-9}	4.8×10^{-10}	---
Sr	5.4×10^{-10}	5.3×10^{-10}	4.8×10^{-10}	4.0×10^{-10}
Ba	2.8×10^{-10}	2.8×10^{-10}	9.8×10^{-10}	5.8×10^{-10}

[a] Indicates whether the reported data for the major
    gases were from a restored or raw gas analysis.
    Analyses of sufficient quality were "improved" using
    a thermodynamic restoration procedure as described
    by Symonds et al. (1990).

[b] Calculated using the average molar ratios of elements
    to H_2O in the gas condensates (Symonds et al., 1990), and
    the mole fraction of H_2O in the gas analyses (above).

--- = below detection or not determined

heterogeneous equilibrium, respectively, in ideal gases. Both codes have been applied previously to volcanic-gas studies (SYMONDS et al., 1987, 1988, 1990; SPYCHER and REED, 1989; BERNARD et al., 1990; SYMONDS, 1990; KODOSKY et al., 1991; SYMONDS and REED, 1992). The programs calculate the distribution of hundreds of gas, solid, and liquid species in systems of up to forty-two components as a function of temperature and pressure using the basic formulations of

equilibrium calculations for aqueous systems of REED (1982), modified (REED and SYMONDS, 1992) for gases. The calculations are constrained by thermochemical data (SYMONDS, 1990; SYMONDS and REED, 1992) and consist of solving simultaneously a series of mass balance and mass action equations using a Newton-Raphson method (REED and SYMONDS, 1992).

Assumptions and Uncertainties

The following calculations assume chemical equilibrium, although the extent to which equilibrium applies to the Augustine volcanic gases is not completely known. Another uncertainty is whether the quality and quantity of the thermochemical data are sufficient to predict the most stable gas, mineral, or liquid species. One reason for doing these calculations is to test these assumptions.

Thermochemical evaluations of high-temperature (>500°C) samples of the major volcanic gases (H_2O, H_2, CO_2, CO, H_2S, SO_2, HCl, HF) have shown they are often quenched equilibrium compositions and that internal equilibrium is locked in, at, or above the measured temperature at the collection site (GERLACH, 1980a,b; GERLACH and CASADEVALL, 1986a). The restorations of the dome-2 and dome-3 samples are consistent with internal equilibrium in those samples, although the samples are not of sufficient quality to completely prove the equilibrium hypothesis (SYMONDS et al., 1990).

The applicability of equilibrium to trace species in high-temperature volcanic gases can be evaluated directly by comparing numerical calculations to analyses of gas condensates (SYMONDS et al., 1987; SYMONDS and REED, 1992). By computing the distribution of trace element gas species in equilibrium with the known or assumed phenocryst assemblage in the source magma, trace metal concentrations in the gas phase can be estimated. If the calculated concentrations (or "volatilities") agree with the analytical data, they support the equilibrium volatility model. Such comparisons at Merapi and Mount St. Helens volcanoes show that equilibrium calculations provide a means to understand the natural process, even though the calculations do not exactly reproduce the observed concentrations of all trace components in the gas phase (SYMONDS et al., 1987; SYMONDS and REED, 1992).

GASEOUS SPECIES ESCAPING FROM THE AUGUSTINE MAGMA

The following calculations are used to determine the probable volatile compounds that issue from Augustine's magma reservoir. We assumed that the Augustine volcanic gases could be represented by the dome-3 composition (Table 1). This assumption is supported by the field observation in July 1986 and August 1987 that more than 90% of the volcanic gas issued in the proximity of the 1986 lava dome, and by the dome-3 gas composition which is the least oxidized of the dome gas samples, and therefore best represents the gas composition prior to atmospheric contact.

For these calculations, we considered 460 gas species (Table 2) for twenty-nine analyzed components: C, O, H, S, Cl, F, Br, Na, K, Fe, Zn, Cd, Al, Cu, Bi, Pb, Mo, As, Sb, Si, Mg, Ca, Ti, Cr, Ni, Mn, V, Sr, and Li.

We have broken the calculations into several steps. First, we calculated the homogeneous (gases only) equilibrium distribution of gas species at the vent conditions of 870°C and 1 atm. Second, we repeated the homogeneous equilibrium calculations at higher temperatures and pressures to evaluate the degassing of subsurface magma. Finally, we did a series of heterogeneous equilibrium (gases, solids, liquids) calculations at 870°C and 1 atm, and at higher temperatures to test if some elements were more concentrated in solids than in gaseous species.

Homogeneous Equilibrium Speciation of Gases at 870°C and 1 Atmosphere

The calculated equilibrium distribution of gas species at the 870°C and 1 atm are shown in Table 2. The results predict that most metals and semimetals in the dome fumarole are transported as simple chloride gas species; NaCl, KCl, $FeCl_2$, $ZnCl_2$, $CaCl_2$, $PbCl_2$, CuCl, $SbCl_3$, $MgCl_2$, LiCl, $MnCl_2$, $TiCl_4$, $NiCl_2$, BiCl, and $SrCl_2$ are the most stable species of their respective components.

However, chlorides are not the most stable species for all trace components in the Augustine volcanic gas. Mo, Cr, V, Si, Al, and As are transported as oxychlorides (MoO_2Cl_2, CrO_2Cl_2, $VOCl_3$), fluorides (SiF_4), oxyfluorides (AlF_2O), and sulfides (AsS). Cadmium is most abundant as the elemental gas, although our calculations do not consider $CdCl_2$, a more plausible dominant species, because it is not in our data base.

Homogeneous Equilibrium Speciation of Gases at Higher Temperatures and Pressures

The calculations were repeated at higher temperatures and pressures because the volcanic gases may come from subsurface magma. JOHNSTON (1978) estimated a maximum temperature of 1050°C for the 1976 Augustine andesite using two-pyroxene geothermometry so we take that as an upper temperature limit. As explained elsewhere (SYMONDS, 1990), we also fixed the fO_2 at higher temperatures at 0.07 log units below the Ni-NiO (NNO) buffer to match the observed fO_2 of the dome-3 sample at 870°C.

Most of the dominant gas species for the twenty-nine components do not change significantly when the gas is heated from 870 to 1050°C, although the abundances of SO_2, H_2, HF, $PbCl_2$, and BiCl increase slightly and $VOCl_3$ decreases (Fig. 3). Si, Mo, and Sb are exceptions; they are transported as $SiOF_2$, H_2MoO_4, and SbS at higher temperatures. In addition, temperature increase causes the secondary species CO, SO, SiO, SiO_2, $Fe(OH)_2$, NaOH, KOH, PbCl, As_2, Zn, As, Sb, Pb, Bi, and VO_2 to become more abundant but not dominant, while H_2S, S_2, S_2O, COS, H_2S_2, S_3, $(NaCl)_2$, $(KCl)_2$, $PbCl_4$, $FeCl_3$, and BiS become less abundant.

To simulate the distribution of species at higher pressures, the calculations were repeated at 1050°C, varying pressure from 1 to 100 atm (Fig. 4). During open-system degassing at Augustine in 1986–87, the actual pressure of the gas at depth was probably less than lithostatic pressure because the gas had an open pathway to the surface. It must also have been greater than atmospheric pressure because volcanic gases
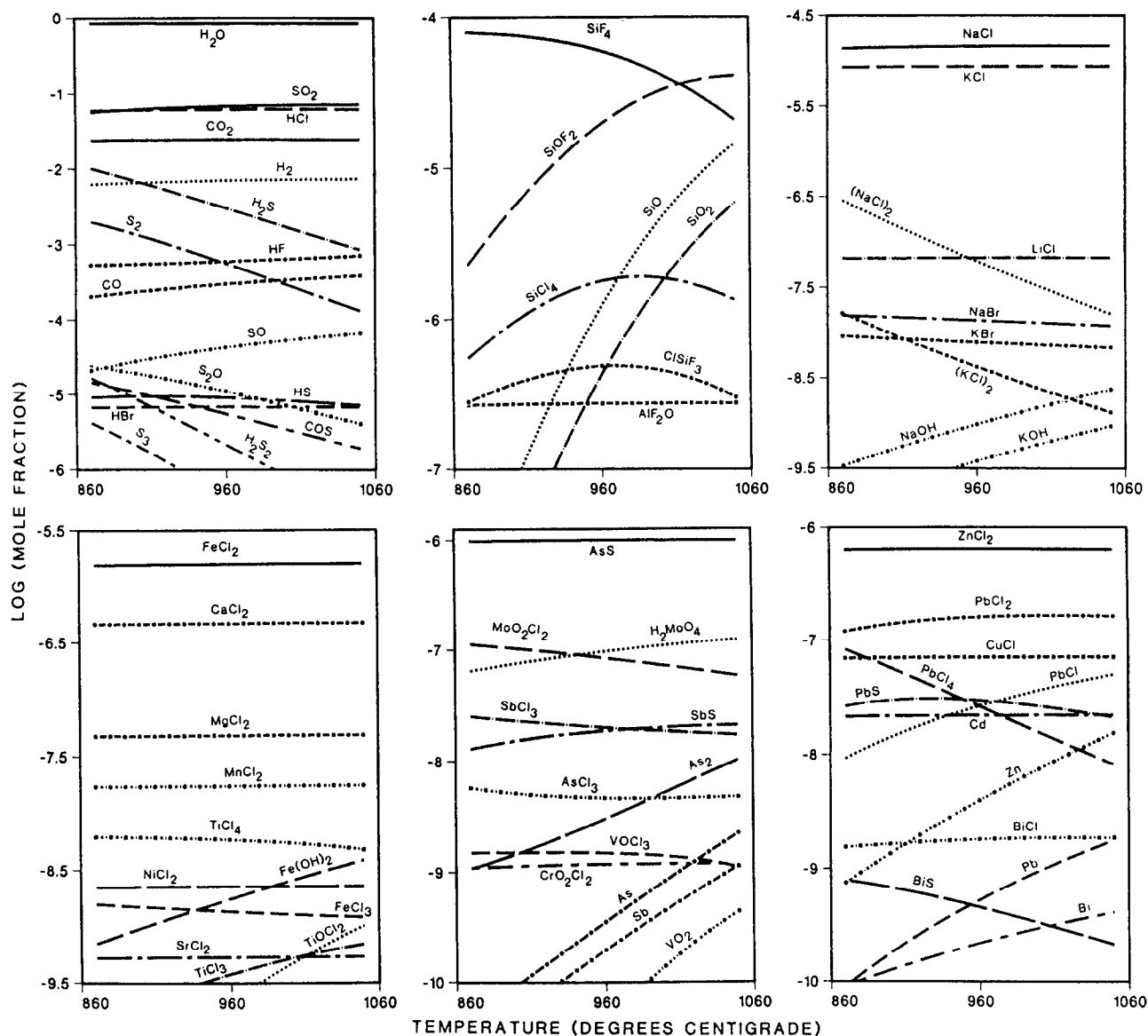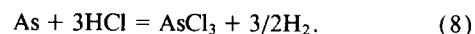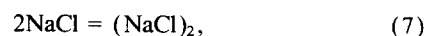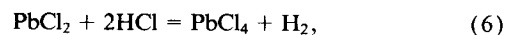
Table 2.   Calculated homogeneous equilibrium distribution of gas species for the dome-3 gas at 870°C and 1 atmosphere (see text). Data are mole fractions listed in order of abundance from top to bottom and left to right.

Quantified species (mole fractions)

Species	Mole fraction	Species	Mole fraction
H₂O	8.4×10^{-1}	S	7.9×10^{-9}
HCl	6.0×10^{-2}	SiF₃	7.3×10^{-9}
SO₂	5.7×10^{-2}	TiCl₄	6.3×10^{-9}
CO₂	2.4×10^{-2}	AsCl₃	6.1×10^{-9}
H₂S	1.0×10^{-3}	S₄	6.0×10^{-9}
H₂	6.2×10^{-3}	H	5.1×10^{-9}
S₂	1.9×10^{-3}	SiO₂	4.1×10^{-9}
HF	5.4×10^{-4}	OH	4.1×10^{-9}
CO	2.0×10^{-4}	Br	3.3×10^{-9}
SiF₄	8.0×10^{-5}	NiCl₂	2.2×10^{-9}
S₂O	2.3×10^{-5}	FeCl₃	1.6×10^{-9}
SO	2.1×10^{-5}	BiCl	1.6×10^{-9}
H₂S₂	1.6×10^{-5}	VOCl₃	1.5×10^{-9}
COS	1.4×10^{-5}	SiCl₃	1.2×10^{-9}
NaCl	1.4×10^{-5}	As₂	1.1×10^{-9}
HS	8.9×10^{-6}	SiHCl₃	1.1×10^{-9}
KCl	8.7×10^{-6}	CrO₂Cl₂	1.1×10^{-9}
HBr	6.8×10^{-6}	AlCl₃	1.0×10^{-9}
S₃	4.1×10^{-6}	CS₂	1.0×10^{-9}
SiOF₂	2.2×10^{-6}	BiS	7.8×10^{-10}
FeCl₂	1.6×10^{-6}	Zn	7.2×10^{-10}
AsS	9.8×10^{-7}	Fe(OH)₂	7.0×10^{-10}
ZnCl₂	6.4×10^{-7}	SrCl₂	5.3×10^{-10}
SiCl₄	5.3×10^{-7}	SiS	4.6×10^{-10}
CaCl₂	4.6×10^{-7}	AlCl₂F	4.0×10^{-10}
(NaCl)₂	2.9×10^{-7}	NaOH	3.3×10^{-10}
ClSiF₃	2.8×10^{-7}	Cl₂	3.0×10^{-10}
AlF₂O	2.7×10^{-7}	S₅	2.7×10^{-10}
PbCl₂	1.2×10^{-7}	SCl	2.3×10^{-10}
MoO₂Cl₂	1.1×10^{-7}	MgClF	1.6×10^{-10}
PbCl₄	8.6×10^{-8}	TiCl₃	1.5×10^{-10}
CuCl	6.9×10^{-8}	KOH	1.3×10^{-10}
LiCl	6.7×10^{-8}	NaF	1.2×10^{-10}
H₂MoO₄	6.5×10^{-8}	SCl₂	1.0×10^{-10}
MgCl₂	4.8×10^{-8}	CuBr	9.6×10^{-11}
Cl	4.3×10^{-8}	Bi	9.1×10^{-11}
SiS₂	3.4×10^{-8}	CrCl₄	8.9×10^{-11}
FSiCl₃	3.3×10^{-8}	Pb	8.7×10^{-11}
SbCl₃	2.6×10^{-8}	KF	5.4×10^{-11}
PbS	2.5×10^{-8}	AlClF₂	5.4×10^{-11}
S₂Cl	2.4×10^{-8}	As	4.7×10^{-11}
Cd	2.1×10^{-8}	HClO	4.0×10^{-11}
MnCl₂	1.7×10^{-8}	LiBr	3.3×10^{-11}
(KCl)₂	1.7×10^{-8}	SiCl₂	2.9×10^{-11}
SiHF₃	1.6×10^{-8}	TiOCl₂	2.9×10^{-11}
NaBr	1.6×10^{-8}	TiF₃	2.5×10^{-11}
SiO	1.3×10^{-8}	Sb	2.4×10^{-11}
SbS	1.2×10^{-8}	LiF	1.3×10^{-11}
SO₃	1.2×10^{-8}	Mg(OH)₂	1.2×10^{-11}
KBr	9.3×10^{-9}	H₂SO₄	1.2×10^{-11}
PbCl	9.0×10^{-9}		

Trace species (listed in order of abundance, with $\leq$ thresholds)

$\leq1\times10^{-11}$	AlFO	TiO₂	(NaOH)₂	MoCl₅	TiBr₄	(SbS)₄	$\leq1\times10^{-40}$
LiOH	SF	SSF₂	AlOH	SrF	C₂H₂	MoF₂	F₂O
AsH₃	MoO₃	AlF₂	(KF)₂	BiBr₃	AlO	(MgBr₂)₂	SiC
BiCl₃	(MgCl₂)₂	MgOH	Mg	(TiCl₃)₂	SiH₃	CF	MoF₆
(HF)₂	Sb₂	Li₂ClF	MgS	MgH		TiBr	(HF)₆
Na	AlOCl	CaCl	NaO	(CuBr)₃	$\leq1\times10^{-24}$	CCl₄	Al₂S
SOCl₂	AlCl₂	PbF₂	MoO₂		CH₂F₂	MoBr	SiC₂
BrCl	Br₂	Cr	SF₂	$\leq1\times10^{-21}$	TiCl	O₃	CBr₄
AlF₃	NiBr	As₄O₆	CaF	SiH₃Br	CH₂	CCl	C₂
Cu	PBF	SbF₃	CH₃	SrBr	CaO	CH	Si₂C
CdS	CS	SrBr₂	Mn	LiO	TiF	MoF₄	C₂F₂
(FeCl₂)₂	S₇	LiAlF₄	$\leq1\times10^{-18}$	SiCH₃F₃	(LiF)₃	MoBr₄	(AlBr₃)₂
Ca(OH)₂		CuF	AlBr₃	LiNaO	MoF		
VCl₄	$\leq1\times10^{-14}$	As₄S₄	SrCl	Pb₂	C₂H₄	SrH	$\leq1\times10^{-45}$
CuH	HCO	COClF	NiH	TiBr₃	LiClO	CCl₃F	Fe(CO)₅
VO₂	Na₂SO₄	BrF	SiH₂Br₂	(FeBr₂)₂	F₂		BrF₃
SiH₂F₂	NiS	$\leq1\times10^{-16}$	(FeCl₃)₂	SiH₄	MoBr₂	Mo	Ca₂
S₆	CHFO	(NaF)₂	VO	SiH₂	(AlO)₂		C₃
(CuCl)₃	FeF₃	MnF₂	AsBr₃	AlBr	$\leq1\times10^{-25}$	AlH₂	AlC
S₂Cl₂	(KBr)₂	CH₃Cl	FS₂F	K₂S	Sr		SF₅
CH₂O	MgBr₂	HO₂	TiOF	SbCl₅	Li₂O	$\leq1\times10^{-30}$	CF₃OF
PbBr	AlO₂H	Fe	COF	TiO	CHCl₂F	MoCl₆	ClF₃
NaAlF₄	PbH	SO₂Cl₂	LiH	(AlF₃)₂	ClO₂	C₂H₄O	(HF)₇
	HSO₃F	SiH₃F	SiBr₂	PbF₄	SrO	FO₂	C₂F₄
$\leq1\times10^{-12}$	AlClF	S₈	Sb₃S₂	MgO	FO	CCl₂F₂	
(LiCl)₂	H₂O₂	SbH₃	SO₂F₂	(MgF₂)₂	CCl₂	Li₂O₂	$\leq1\times10^{-50}$
CaF₂	CrO₃	SrF₂	(BiS)₂	SiBr₃	CHCl	CBr	ClO₂F
SiF₂	MnBr₂	AlF	(LiBr)₂	BiF₃	K₂	VF₅	Si₃
NiCl	MoCl₄	BiF	(KOH)₂	SiHBr₃	TiS	C₂Cl₂	C₂Cl₆
FeBr₂	CrO	Ni	CuF₂	CH₂ClF	CHF	CClF₃	SClF₅
K	O	Bi₂	SiCl		CHClF₂	LiFO	ClF₅S
ZnBr₂	TiOF₂	MgF	$\leq1\times10^{-22}$	CaH	Ti	SF₆	
CrO₂	Sb₂S₄	Li	$\leq1\times10^{-19}$	Ca	(HF)₄	C	BrSF₅
As₄	FeS	SiH₃Cl	NiF	SiBr	MoF₃	CF₄	C₂F₆
SiH₂Cl₂	(SbS)₂	FeF	(HF)₃	SiCH₃Cl₃	V	Li₂	
MgF₂	NaH	S₂Br₂	KO	AlO₂	C₃O₂	Ni(CO)₄	$\leq1\times10^{-60}$
O₂		TiOCl	CaBr	Sb₄O₆	Sb₄S₃	CF₃	C₄
PbO	$\leq1\times10^{-15}$	AlCl	Bi₂S₃	Cl₂O	MoBr₃	AlH₃	C₆H₆
As₃	ClO	MgBr	(LiOH)₂	MoO	Al	Al₂O	Si(CH₃)₄
COCl	K₂SO₄	KH	SiF	Na₂	MoOF₄	C₂HF	C₅
ZnS	MgCl	COF₂	Li₂SO₄	SrS		AsF₅	
TiF₄	TiF₂		CH₂Cl₂	CrBr₄	$\leq1\times10^{-27}$	(HF)₅	$\leq1\times10^{-70}$
PbBr₂	CuO	$\leq1\times10^{-17}$	CH₃F		C₂HCl	SF₄	CSF₈
Sb₂S₃	NiBr₂	SOF₂	NiO	$\leq1\times10^{-23}$	CF₂		BrF₅
	TiCl₂	CaOH	(AlCl₃)₂	SiBr₄	HAlO	$\leq1\times10^{-35}$	
$\leq1\times10^{-13}$	AsF₃	TiCl₂	(LiF)₂	(LiCl)₃	(SbS)₃	AlH	MoF₅	$\leq1\times10^{-80}$
CaBr₂	COCl₂	PbBr₄	CaS	SiH	CCl₃	CBrF₃	ClF₅
CH₄	Sr(OH)₂	ClF	Sb₄	C₂H₆	Mg₂		
(NaBr)₂	FeF₂	SO₂ClF	$\leq1\times10^{-20}$	Si	VBr₄	C₂Cl₄	$\leq1\times10^{-90}$
KS	FeCl	SbBr₃	SrOH	AlS	SF₃	Si₂	S₂F₁₀
SBr₂	F	NiF₂	TiBr₂	CHCl₃	CHF₃	(AlS)₂	

escaped forcefully from the dome fumaroles. We assume 100 atm, corresponding to a lithostatic pressure depth of 360 m, to be an upper limit of the pressure of the gas after it left the magma. 1050°C was used because it is the upper limit of the magma temperature.

Increasing pressure causes only a few changes in the dominant gas species for the twenty-nine components, but affects greatly the abundances of many trace species. For the C-O-H-S-F-Cl system, higher pressures cause the mole fractions of H₂S, S₂, S₂O, COS, and H₂S₂ to increase, whereas the mole fractions of H₂, HF, CO, and SO decrease (Fig. 4). For the trace components, higher pressures favor SiF₄ over SiOF₂, AsCl₃ over AsS, SbCl₃ over SbS, and PbCl₄ over PbCl₂. Higher pressures also cause the abundances of SiCl₄, ClSiF₃, FSiCl₃,
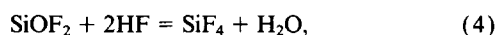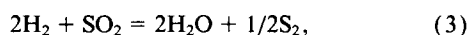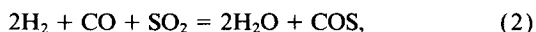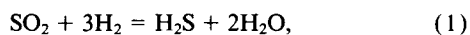
FIG. 3. Calculated homogeneous equilibrium distribution of the most abundant gas species of major and trace components in the Augustine dome-3 sample from 870 to 1050°C and 1 atmosphere pressure. Calculations assume that fO_2 is buffered by the magma 0.07 log units below Ni-NO. Only the more abundant species of each component are shown.

$(NaCl)_2$, $(KCl)_2$, $FeCl_3$, $VOCl_3$, $CrCl_4$, and $BiCl_3$ to increase, whereas the abundances of SiO, SiO_2, $TiOCl_2$, $TiCl_3$, As_2, As, Sb, VO_2, PbCl, PbS, Zn, BiCl, Pb, Bi, and BiS decrease. Such trends are the result of entropy effects wherein higher pressures favor the right sides of reactions that produce fewer moles of product species than there are moles of reactants; for example,

$$SO_2 + 3H_2 = H_2S + 2H_2O, \tag{1}$$

$$2H_2 + CO + SO_2 = 2H_2O + COS, \tag{2}$$

$$2H_2 + SO_2 = 2H_2O + 1/2S_2, \tag{3}$$

$$SiOF_2 + 2HF = SiF_4 + H_2O, \tag{4}$$

$$AsS + 3HCl = AsCl_3 + H_2S + 1/2H_2, \tag{5}$$

$$PbCl_2 + 2HCl = PbCl_4 + H_2, \tag{6}$$

$$2NaCl = (NaCl)_2, \tag{7}$$

$$As + 3HCl = AsCl_3 + 3/2H_2. \tag{8}$$
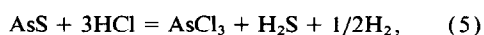
The listed calculations (Figs. 3–4) show that most of the dominant species at 870°C and 1 atm also prevail at higher temperatures and pressures. The species changes caused by increased pressure (Fig. 4) generally oppose the species changes caused by increased temperature (Fig. 3) and suggest that the abundances of $SiOF_2$, SbS, AsS, SO_2, H_2, HF, CO, SO, SiO, SiO_2, PbCl, As_2, Zn, As, Sb, $PbCl_2$, Pb, BiCl, Bi, and VO_2 computed by the 1 atm and 870°C calculations are overestimates for subsurface magma degassing. Thus, the speciation of the gas that escapes from the subsurface
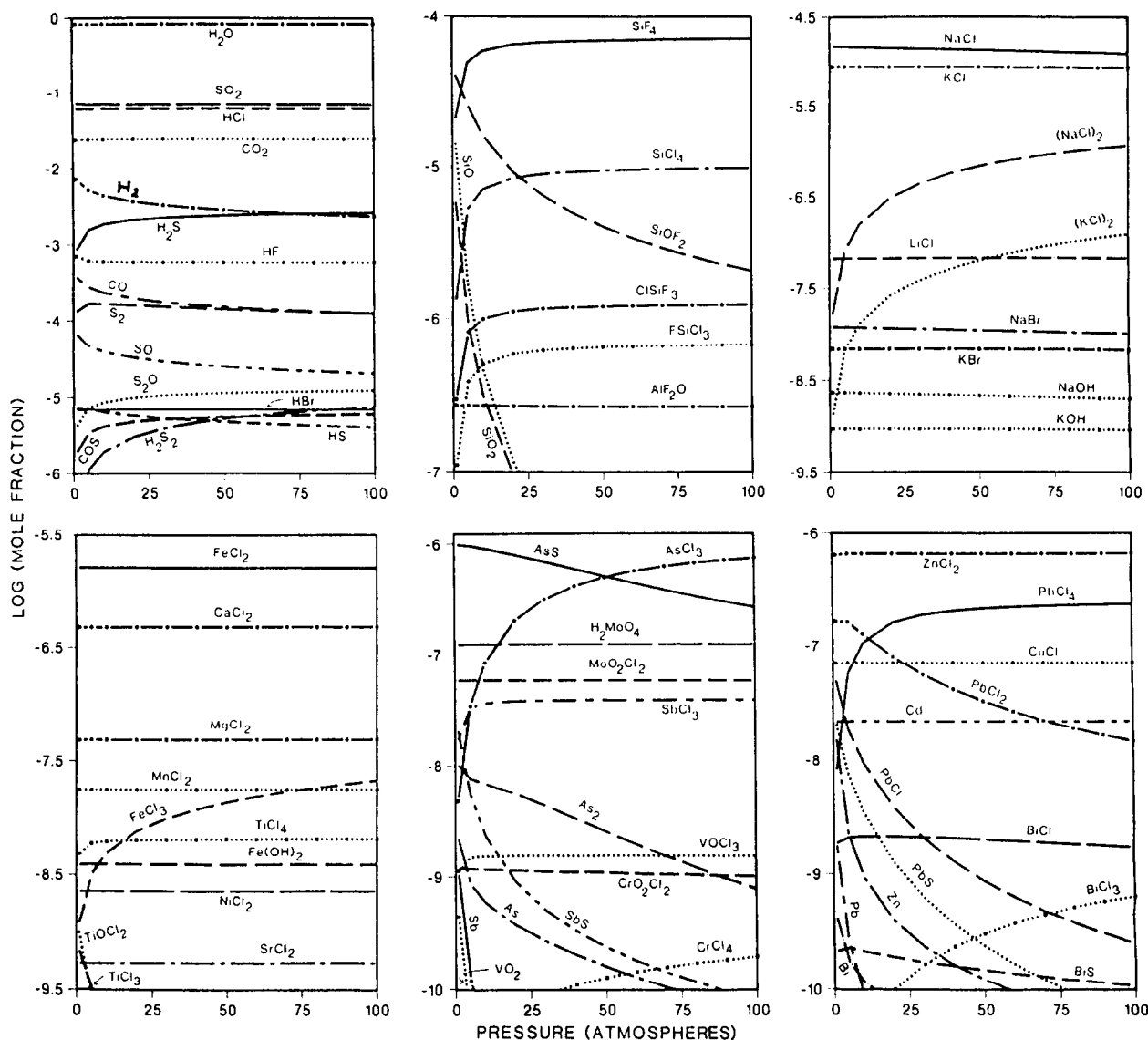
FIG. 4. Calculated homogeneous equilibrium distribution of the most abundant gas species of major and trace components in the Augustine dome-3 sample from 1 to 100 atmospheres and 1050°C. The fO_2 was fixed at 0.07 units below the Ni-NO reference buffer at 1 atm pressure and then calculated by those mass balance constraints at higher pressures. Only the more abundant species of each component are shown.

Augustine magma is better approximated by the 870°C and 1 atm calculations than by the 1050°C and 1 atm calculations.

Heterogeneous Equilibrium Speciation of Gases and Particles at 870 to 1050°C

Homogeneous equilibrium calculations do not account for possible particulate phases that may have dissolved in our condensate samples and thereby biased the above results. Particles may be sublimates precipitated from the volcanic gas (SYMONDS et al., 1987), rock particles eroded from the fumarole walls (QUISEFIT et al., 1988), acidic droplets that condensed on and reacted with the fumarole walls, or condensed species that formed from mixing of cation-bearing waters with the volcanic gas.

To evaluate the possibility of solids and liquids in the volcanic gas, we did a series of heterogeneous equilibrium calculations using the program GASWORKS, taking into account 322 solids and liquids. The calculations were done at 870°C and 1 atm and at higher temperatures using the same assumptions as for the homogeneous equilibrium cases, except that the program was allowed to equilibrate with supersaturated solids or liquids (only pure phases were considered).

The distribution of gas and particle species at 870°C and 1 atm are shown in Table 3. At that temperature, Si, Ca, Al, Mg, Ti, V, and Cr are concentrated more in solids, beta-quartz, wollastonite, anorthite, diopside, sphene, $V_2O_3(c)$, and $Cr_2O_3(c)$ than in gaseous species. As a result, the mole fractions of SiF_4, $CaCl_2$, AlF_2O, $MgCl_2$, $TiCl_4$, $VOCl_3$, and CrO_2Cl_2 have decreased relative to the homogeneous equi-

Table 3. Calculated heterogeneous equilibrium distribution of gas and solid species for the dome-3 gas at 870°C and 1 atmosphere (see text). Only the more abundant species are listed. Solids are identified by mineral names or as crystalline solids (c).

Gas Species (mole fraction)

H_2O	8.4×10^{-1}	$SbCl3$	2.6×10^{-8}
HCl	6.0×10^{-2}	PbS	2.5×10^{-8}
SO_2	5.7×10^{-2}	S_2Cl	2.4×10^{-8}
CO_2	2.4×10^{-2}	Cd	2.1×10^{-8}
H_2S	1.0×10^{-3}	$MnCl_2$	1.7×10^{-8}
H_2	6.1×10^{-3}	$(KCl)_2$	1.7×10^{-8}
S_2	1.9×10^{-3}	$NaBr$	1.6×10^{-8}
HF	8.6×10^{-4}	SbS	1.2×10^{-8}
CO	2.0×10^{-4}	SO_3	1.2×10^{-8}
S_2O	2.3×10^{-5}	$CaCl_2$	9.4×10^{-9}
SO	2.1×10^{-5}	KBr	9.3×10^{-9}
H_2S_2	1.6×10^{-5}	$PbCl$	9.0×10^{-9}
COS	1.4×10^{-5}	S	7.9×10^{-9}
$NaCl$	1.4×10^{-5}	$AsCl_3$	6.1×10^{-9}
HS	8.9×10^{-6}	S_4	6.0×10^{-9}
KCl	8.7×10^{-6}	H	5.1×10^{-9}
HBr	6.8×10^{-6}	$MgCl_2$	4.7×10^{-9}
S_3	4.1×10^{-6}	OH	4.1×10^{-9}
$FeCl_2$	1.6×10^{-6}	Br	3.3×10^{-9}
AsS	9.8×10^{-7}	$NiCl_2$	2.2×10^{-9}
$ZnCl_2$	6.4×10^{-7}	$FeCl_3$	1.6×10^{-9}
$(NaCl)_2$	2.9×10^{-7}	$BiCl$	1.6×10^{-9}
$PbCl_2$	1.2×10^{-7}	AlF_2O	1.1×10^{-9}
MoO_2Cl_2	1.1×10^{-7}	As_2	1.1×10^{-9}
$PbCl_4$	8.6×10^{-8}	CS_2	1.0×10^{-9}
$CuCl$	6.9×10^{-8}	BiS	7.8×10^{-10}
$LiCl$	6.7×10^{-8}	Zn	7.2×10^{-10}
H_2MoO_4	6.5×10^{-8}	$Fe(OH)_2$	7.0×10^{-10}
Cl	4.3×10^{-8}	$SrCl_2$	5.3×10^{-10}

Solids (moles per 1 mole of gas)

beta-quartz	8.2×10^{-5}	sphene	6.5×10^{-9}
anorthite	1.3×10^{-7}	$V_2O_3(c)$	6.6×10^{-10}
wollastonite	2.7×10^{-7}	$Cr_2O_3(c)$	5.9×10^{-10}
diopside	4.3×10^{-8}		

librium case (Table 2). The abundance of HF increases because of the redistribution of F after the breakdown of SiF_4. Heterogeneous equilibrium calculations at higher temperatures show that these same particles are stable up to 1050°C, except that beta-quartz is replaced by beta-tridymite (SiO_2) at 871°C and diopside evaporates into the gas at 1005°C (Fig. 5).

The calculated concentrations of Si, Ca, Al, Mg, Ti, V, and Cr in solids suggests several possibilities:

1) The computed solids may actually be present in the gas, having formed by sublimation in the gas stream.

2) The computed solids may have been supersaturated in the gas phase but did not nucleate due to kinetic effects.

3) The thermodynamic data may be incorrect or incomplete for the gas species of these elements.

4) The elements in solids may originate from the wall rock (process 2, 3, or 4 in Fig. 2) or from contamination (of Si) from the sampling apparatus.

The computed existence of solids of Ca, Al, Ti, and V up to 1050°C, the maximum magma temperature estimate of JOHNSTON (1978), suggests that if these solids actually existed in the gas, they were not sublimates; if the magma was less than 1005°C, diopside was also not a sublimate. This is consistent with the absence of Ca, Al, Ti, V, and Mg sublimates in silica-tube sublimates collected from the dome vent (Symonds, unpubl. data) and with the generally low Mg enrichment factors for Ca, Al, Ti, and V in the dome condensates (SYMONDS et al., 1990). Thus, we favor a wall-rock source (process 2, 3, or 4 in Fig. 2) for Ca, Al, Ti, and V; Mg may
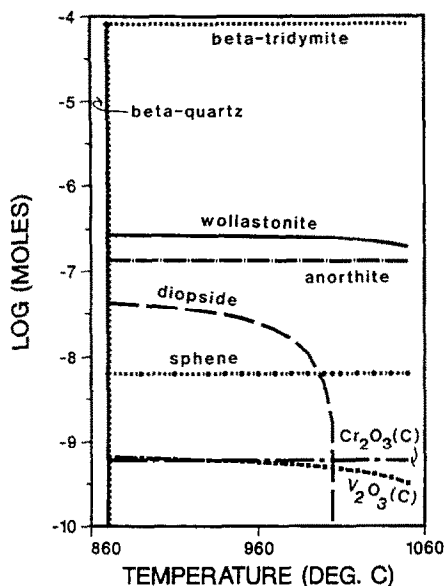
FIG. 5. Calculated distribution of solids in heterogeneous equilibrium with the dome-3 composition (Table 1) from 870 to 1050°C and 1 atmosphere pressure. Calculations assume that $f O_2$ is buffered by the magma 0.07 log units below Ni-NO. Data are in log moles per 1 mole of gas initially introduced.

also come from the wall rock but also could have a volatile component (see following discussion).

Reaction of condensed acid droplets with the wall rock (process 4, Fig. 2) is not possible in the dome vents because sulfuric acid liquids are grossly undersaturated with the dome gases at the vent temperature of 870°C (see below). The fact that Ca, Al, Ti, V, and Mg are computed to be more concentrated in solids than in gaseous species, even in the high-temperature HCl-rich dome gases, suggests that boiling of any reacted meteoric water (with sufficient amounts of Ca, Al, Ti, V, and Mg to contaminate the bulk gas) into the gas stream (process 3, Fig. 2), would not add enough gaseous Ca, Al, Ti, V, and Mg to the bulk gas to explain the observed concentrations. Instead, it would cause precipitation of solids of Ca, Al, Ti, V, and Mg, and they might remain in the wall rock, preventing such elements from contaminating the gas. Furthermore, in the unlikely event that the reacted liquid boiled directly into the gas stream, without first precipitating solids, we should find quenched solids of Ca, Al, Ti, V, and Mg in the dome sublimates, but no such phases have been found (Symonds, unpubl. data).

Thus, we contend that wall-rock erosion is the most viable source of Ca, Al, Ti, V, and possibly Mg in the dome condensates. Rock particles containing these elements were eroded from the fumarole walls, entrained in the gas stream, and dissolved in the condensates. Wall-rock erosion is consistent with studies of particles collected in plumes from passively degassing volcanoes and in fume from volcanic fumaroles. All work to date has shown that refractory elements (e.g., Mg, Al, Ca, Ti, V) are concentrated in silicate rock fragments (e.g., ash) or common igneous minerals (e.g., diopside; ROSE et al., 1982, 1986; VAREKAMP et al., 1986; QUISEFIT et al., 1989).

However, the high enrichments of Si and Cr in the dome condensates (SYMONDS et al., 1990) suggests that these elements did not come from rock particles that contaminated the samples. Instead, Si may have come from dissolution of the silica sampling tube or our program might be missing the dominant gas species of Si.

Also, the dominant Cr species might be missing from our model (see below). Since Ca, Al, Mg, Ti, and V probably came from eroded rock particles and Si may have come from reaction with the silica sampling tube, Table 3 is our "best" estimate of the distribution of gas species in the Augustine volcanic gas at 870°C and 1 atm. The molecular form of the gas is likely to be similar even if the degassing magma is somewhat below the surface, as explained earlier. It is possible, however, that additional trace elements (e.g., Sr) came from dissolved rock particles that were not accounted for by our model, which only considers pure solids (e.g., SrSiO₃, SrSiO₄).

Comparison with Other Volcanoes

We restrict comparison of the Augustine results to our own calculations for Mount St. Helens (SYMONDS, 1990; SYMONDS and REED, 1992) and Merapi (SYMONDS et al., 1987). In general, the predicted molecular form of the Augustine volcanic gases at magmatic conditions is similar to Mount St. Helens and Merapi, taking into account that the Mount St. Helens gases were not analyzed for Si and Mg and that the Merapi calculations did not allow for heterogeneous equilibration with supersaturated solids of Al, Mg, V, and Cr. The major differences at 870-930°C and 1 atm pressure are as follows:

1) Molybdenum is transported as MoO_2Cl_2 at Augustine but as H_2MoO_4 at Merapi and Mount St. Helens.
2) Lead is dominated by $PbCl_2$ at Augustine but by PbS at Merapi and Mount St. Helens.
3) Bismuth is volatilized as BiCl at Augustine but as BiS and the elemental gas at Merapi and Mount St. Helens, respectively.
4) Zinc is carried as a chloride, $ZnCl_2$, at Augustine and Merapi but as the elemental gas at Mount St. Helens.
5) Iron is most stable as $FeCl_2$ at Augustine but as $Fe(OH)_2$ at Mount St. Helens.
6) Antimony is transported as $SbCl_3$ at Augustine but as SbS at Mount St. Helens.

The above comparison demonstrates that chloride species, MoO_2Cl_2, $PbCl_4$, BiCl, $ZnCl_2$, $FeCl_2$, and $SbCl_3$ are more abundant in HCl-rich gases like those of Augustine. However, in volcanic gases that have less HCl, such as those from Mount St. Helens and Merapi, the trace metals are more likely to be transported as oxyacid, sulfide, elemental, and hydroxide gas species.

GEMMELL (1987) suggests that bromides could play a role in the transport of metals in volcanic gases because metal bromides are intrinsically more stable than their respective chlorides. However, thermochemical modeling for Augustine (Tables 2-3, Figs. 3-4) shows that metal bromides are not very abundant compared to metal chlorides, oxychlorides, sulfides, hydroxides, or elemental species in high-temperature volcanic gases. This also applies to volcanic gases from Mer-

api, Mount St. Helens, Etna, and Momotombo (SYMONDS et al., 1987; LE GUERN, 1988; QUISEFIT et al., 1989; SYMONDS, 1990; SYMONDS and REED, 1992). Thus, it appears that bromides, despite their intrinsic stability, do not play a significant role in metal transport in volcanic gases because bromine is much less concentrated than chlorine in the bulk gas.

FLUXES OF GAS SPECIES

The distribution of species as calculated from GAS-WORKS and the correlation spectrometry (COSPEC) SO_2 fluxes (ROSE et al., 1988; SYMONDS et al., 1990) can be used to estimate fluxes of many species in the Augustine plume. The basic equation is as follows:

$$F_j = R_j \times F_s \times M_j \qquad (9)$$

where F_j is the flux of species, j, in g/day; R_j is the molecular ratio of the jth species to SO_2; F_s is the sulfur dioxide flux in moles per day; and M_j is the molecular weight of the species, j.

R_j values were estimated using the heterogeneous equilibrium distribution of SO_2 and other species at 870°C for the dome-3 gas (Table 3). Fluxes were estimated for each day that COSPEC data were collected including measurements for passive degassing (SYMONDS et al., 1990) and low-level eruptive activity (ROSE et al., 1988). We used the same R_j values, those calculated using the dome-3 composition of 28 August 1987, for all flux determinations. This was done because dome-3 is our best estimate of the bulk volcanic gas that issued from Augustine over this time period and not meant to imply that the R_j values might not have changed over our two-year study. Nonetheless, our estimates should give some indication of how the fluxes of species might have changed over this time period.

The fluxes are estimates of the rates of transport of the computed gas species away from high-temperature fumaroles. As the gases enter and mix with the atmosphere, however, their molecular form (and the resulting fluxes) may change as they cool, condense, and oxidize. More complex calculations, which are beyond the scope of this paper, are needed to model the speciation of volcanic gases as they mix and react with the atmosphere.

Emission rates for the more abundant gas species, including many species that have not been considered previously at active volcanoes, are reported in Table 4. We do not report fluxes for species of Si, Ca, Al, Mg, Ti, V, and Cr because the speciation results for these elements are unreliable. The estimated emission rates of gas species decrease by three orders of magnitude from the low-level eruptive rates for 3 April 1986 to the passive degassing rates of August 1987, reflecting the decrease in SO_2 emission rates (Table 4). Future studies should make such estimates for other volcanoes; eventually, we could project the global volcanic fluxes of many important species.

ROSE et al. (1988) report an HCl flux of 10,000 Mg/day for 3 April 1986, which is similar to our estimate (Table 4) of 14,000 Mg/day. However, the previous estimate of 8000 Mg/day for the HCl flux for 24 July 1986 by ROSE et al. (1988) is now revised to 230 Mg/day. The prior estimate

was made using Cl/S ratios from condensate analyses because the gas analyses (SYMONDS et al., 1990) were not yet available. This new estimate is still one of the highest HCl fluxes reported for passively degassing volcanoes (SYMONDS et al., 1988).

The above flux estimates assume that no oxidation of S species occurred in the plume. Because COSPEC measurements are made on the volcanic plume and some of the measured SO_2 probably comes from atmospheric oxidation of reduced S species such as H_2S (JAESCHKE et al., 1982), it is possible that the above fluxes (Table 4) are overestimates. To test the effect of oxidation of S in the plume, the fluxes were recomputed assuming all the S in the plume was present as SO_2. The resulting fluxes (SYMONDS, 1990) are about 20% less than those reported in Table 4, which is within the uncertainty of our flux estimates.

GAS-ANDESITE TITRATIONS

The above calculations suggest that at magmatic conditions most elements in the Augustine dome fumarole emissions occur as gaseous species, probably volatilized from magma. However, Ca, Al, Mg, Ti, V, Cr, and Si are calculated to exist as solids, indicating contaminated condensates or incorrect predictions of our model.

To discriminate between volatilization and other processes in the dome and moat fumaroles, we did a series of numerical titrations of andesite into volcanic gas using the heterogeneous equilibrium program GASWORKS. In the numerical titrations, we take fixed amounts of each of several major gas compositions (trace elements excluded, except Br) and titrate them with rock of a specific composition until the mole fractions of trace components in the gas are buffered by a stable mineral assemblage. This is a new approach to volatility calculations. By comparing our computed volatilities with compositions of condensate samples, we can test whether our samples were once in equilibrium with the magma, and if so, the minimum amount of magma necessary to buffer each trace element. Calculation results also aid in assessing the role of erosion, leaching, or acid attack in instances where simple volatilization fails to explain the observed concentrations of elements in the gas phase.

Assumptions and Reaction Steps

We have no independent means of estimating compositions of the major gases expelled from the Augustine magma. We assume, for the purposes of these volatility calculations, that the concentrations of the major gases (H_2O, HCl, SO_2, CO_2, H_2S, H_2, S_2, HF, CO, HBr) determined from samples were buffered by magma or, at least, that major gas concentrations are so large relative to trace gases that they are not significantly changed by magma reaction. In accordance with these assumptions, we hold the major gas concentrations at fixed values during the rock titrations, then compute the trace gas concentrations in a hypothetical volatilization process.

The calculations are broken into several steps: (1) reaction of 1986 andesite (Table 5) with the dome-3 gas (Table 1) at the vent temperature of 870°C until the gas saturates with a stable equilibrium mineral assemblage; (2) repeating the

Table 4. Estimated fluxes (grams/day) of some the
more abundant gas species that are
possibly emitted from Augustine volcano
(see text). SO_2 fluxes measured directly
by COSPEC by Rose et al. (1988) for
4/3/86 and by Symonds et al. (1990) for
all other dates. Other fluxes estimated
using the calculated distribution of gas
species (Table 3) and the COSPEC data.

Date:	4/3/86	7/24/86	5/24/87	8/24/87
Uncertainty[*]:	±17%	±60%	±60%	±22%
H_2O	9.9×10^{11}	1.6×10^9	1.9×10^8	1.1×10^8
SO_2	2.4×10^{10}	3.8×10^8	4.5×10^7	2.7×10^7
HCl	1.4×10^{10}	2.3×10^8	2.7×10^7	1.6×10^7
CO_2	6.9×10^9	1.1×10^8	1.3×10^7	7.8×10^6
H_2S	2.2×10^9	3.6×10^7	4.2×10^6	2.5×10^6
S_2	8.2×10^8	1.3×10^7	1.5×10^6	9.2×10^5
HF	1.1×10^8	1.8×10^6	2.1×10^5	1.3×10^5
H_2	8.1×10^7	1.3×10^6	1.5×10^5	9.1×10^4
CO	3.7×10^7	5.8×10^5	6.9×10^4	4.1×10^4
S_2O	1.2×10^7	1.9×10^5	2.3×10^4	1.4×10^4
H_2S_2	7.0×10^6	1.1×10^5	1.3×10^4	7.9×10^3
SO	6.5×10^6	1.0×10^5	1.2×10^4	7.3×10^3
COS	5.6×10^6	8.9×10^4	1.1×10^4	6.3×10^3
$NaCl$	5.3×10^6	8.4×10^4	1.0×10^4	6.0×10^3
KCl	4.2×10^6	6.7×10^4	8.0×10^3	4.8×10^3
HBr	3.6×10^6	5.7×10^4	6.7×10^3	4.0×10^3
S_3	2.6×10^6	4.1×10^4	4.8×10^3	2.9×10^3
HS	1.9×10^6	3.1×10^4	3.6×10^3	2.2×10^3
$FeCl_2$	1.3×10^6	2.1×10^4	2.5×10^3	1.5×10^3
AsS	6.9×10^5	1.1×10^4	1.3×10^3	780.
$ZnCl_2$	5.7×10^5	9.0×10^3	1.1×10^3	640.
$PbCl_2$	2.2×10^5	3.4×10^3	410.	240.
$PbCl_4$	2.0×10^5	3.1×10^3	370.	220.
MoO_2Cl_2	1.5×10^5	2.3×10^3	280.	170.
H_2MoO_4	6.9×10^4	1.1×10^3	130.	77.
$CuCl$	4.5×10^4	710.	84.	51.
PbS	3.9×10^4	620.	74.	44.
$SbCl_3$	3.9×10^4	620.	74.	44.
$LiCl$	1.9×10^4	290.	35.	21.
Cd	1.6×10^4	250.	30.	18.
$MnCl_2$	1.4×10^4	230.	27.	16.
SbS	1.3×10^4	200.	24.	14.
$BiCl$	2.5×10^3	40.	4.7	2.8
$NiCl_2$	1.9×10^3	30.	3.6	2.1
BiS	1.2×10^3	20.	2.3	1.4
$SrCl_2$	550.	8.7	1.0	0.6

[*]Uncertainty in the fluxes due to one standard
deviation in the COSPEC data. Values for 7/24/86
and 5/24/87 are modified from Symonds et al. (1990)
to take into account the large uncertainty in the
windspeed measurements on those days.

above at higher temperatures, as the magma may be hotter than 870°C; and (3) reaction of andesite with the 642°C moat-4 gas (Table 5) at a range of oxygen fugacity conditions to evaluate metal transport in the oxidized moat vents.

As gas is titrated with rock, the gas/rock (G/R) ratio decreases. At each incremental addition of rock, GASWORKS calculates the equilibrium mineral assemblage for that bulk composition. Because the 1976 and 1986 Augustine andesites contain plagioclase, augite, orthopyroxene, olivine, and

magnetite-ulvöspinel (JOHNSTON, 1978; HARRIS et al., 1987), we assume ideal, multisite mixed solid solutions exist between (1) anorthite, albite ($NaAlSi_3O_8$), and high-sanidine ($KAlSi_3O_8$); (2) diopside, hedenbergite ($CaFeSi_2O_6$), and jadeite ($NaAlSi_2O_6$); (3) orthoenstatite ($MgSiO_3$) and orthoferrosilite ($FeSiO_3$); (4) forsterite (Mg_2SiO_4), fayalite (Fe_2SiO_4), tephroite (Mn_2SiO_4), and Ni_2SiO_4; and (5) magnetite (Fe_3O_4) and ulvöspinel (Fe_2TiO_4). We also suppress the formation of Cr_2O_3(c) (Fig. 5) because it is not a mineral.

Table 5. Assumed major and trace element composition of
          the 1986 Augustine andesite for modeling in this
          paper. Only elements that are actually used in
          the titrations are reported. Listed in order of
          decreasing abundance.

Major Elements (wt %)		Source
SiO_2	61.36	1
Al_2O_3	16.83	1
CaO	6.82	1
FeO	5.38	1
Na_2O	3.65	1
MgO	3.56	1
K_2O	0.98	1
TiO_2	0.55	1
MnO	0.12	1
Trace Elements (ppm)		
Ba	864	2
Sr	300	2
Zn	111	2
Cu	46	3
Ni	37	4
Cr	23	2
As	3.04	2
Sb	1.12	2

[1] average 1986 whole rock from Swanson and Kienle (1988)
[2] 1986 ash (sample Ash A) from Rose et al. (1988)
[3] 1976 ash from Lepel et al. (1978)
[4] 1986 unaltered ash from Kodosky and Keskinen (1990)

Gas-Andesite Titrations at 870°C and 1 Atmosphere

Figure 6 shows the calculated results for reacting the 1986 Augustine andesite with the dome-3 gas composition. These calculations were started at a G/R weight ratio of 1000; higher G/R ratios seem unlikely even in the Augustine fumaroles. Although the calculations were completed to a G/R ratio of 0.01, we only display (Fig. 6) the reaction progress down to a G/R ratio of 1.0 because at that point the gas trace element concentrations are effectively buffered by the large mineral assemblage; additions of more rock do not modify significantly this mineral assemblage and the computed volatilities.

At a log gas/rock (LG/R) ratio of 3, the equilibrium mineral assemblage consists of beta-quartz, Ca-rich plagioclase (anorthite, albite, sanidine), Mg-rich orthopyroxene (orthoenstatite, orthoferrosilite), rutile (TiO_2), cordierite ($Mg_2Al_4Si_5O_{18}$), and picrochromite ($MgCr_2O_4$). Cordierite evaporates into the gas at a LG/R ratio of 2.6. At a LG/R ratio of 2.4, sphene forms; it becomes the main Ti phase as rutile evaporates into the gas below a LG/R ratio of 2.3. Clinopyroxene (diopside, hedenbergite, jadeite) starts precipitating at a LG/R ratio of 2.2. Mg-rich olivine (forsterite, fayalite, tephroite, Ni_2SiO_4) saturates at a LG/R ratio of 1.9. Finally, at a LG/R ratio of 1.1, bornite (Cu_5FeS_4) forms. As more rock is added, this final mineral assemblage does not change significantly, at least until the calculations were terminated at a LG/R ratio of −2.

In detail, some mineral compositions change in the course of the titration. The mole fractions of ferrosilite in orthopyroxene, and albite and sanidine in plagioclase, increase while the G/R ratio decreases from 1000 to 1 (Fig. 6). These changes are the result of the more volatile Fe, Na, and K being extracted preferentially from the rock at high G/R ratios and could reflect possible effects on phenocryst compositions of rock in systems where the G/R ratio is high (e.g., volcanic fumaroles, lava tubes). Since Mg is less volatile than Fe, the mole fraction of orthoenstatite in orthopyroxene increases at higher G/R ratios. Similarly, the mole fraction of anorthite increases at high G/R ratios as Na and K are volatilized from plagioclase.

At very high G/R ratios, the concentrations of trace elements in the gas phase increase as more rock is added (Fig. 6). At lower G/R ratios, however, changing mineral assemblages govern the concentrations of trace elements until the final equilibrium assemblage forms (at a LG/R ratio of 1.1), after which the concentrations of trace elements in the gas phase are stable even as more rock is added to the gas (Fig. 6). Thus, the concentrations of NaCl and KCl increase until the mole fractions of albite and sanidine in plagioclase stabilize. $MnCl_2$ and $NiCl_2$ increase with decreasing G/R ratios until the composition of olivine stops changing at LG/R ratios below 1.9. $MgCl_2$ and $FeCl_2$ are controlled by beta-quartz and the specific composition of orthopyroxene at all G/R ratios considered. Below a LG/R ratio of 2.2, the mole
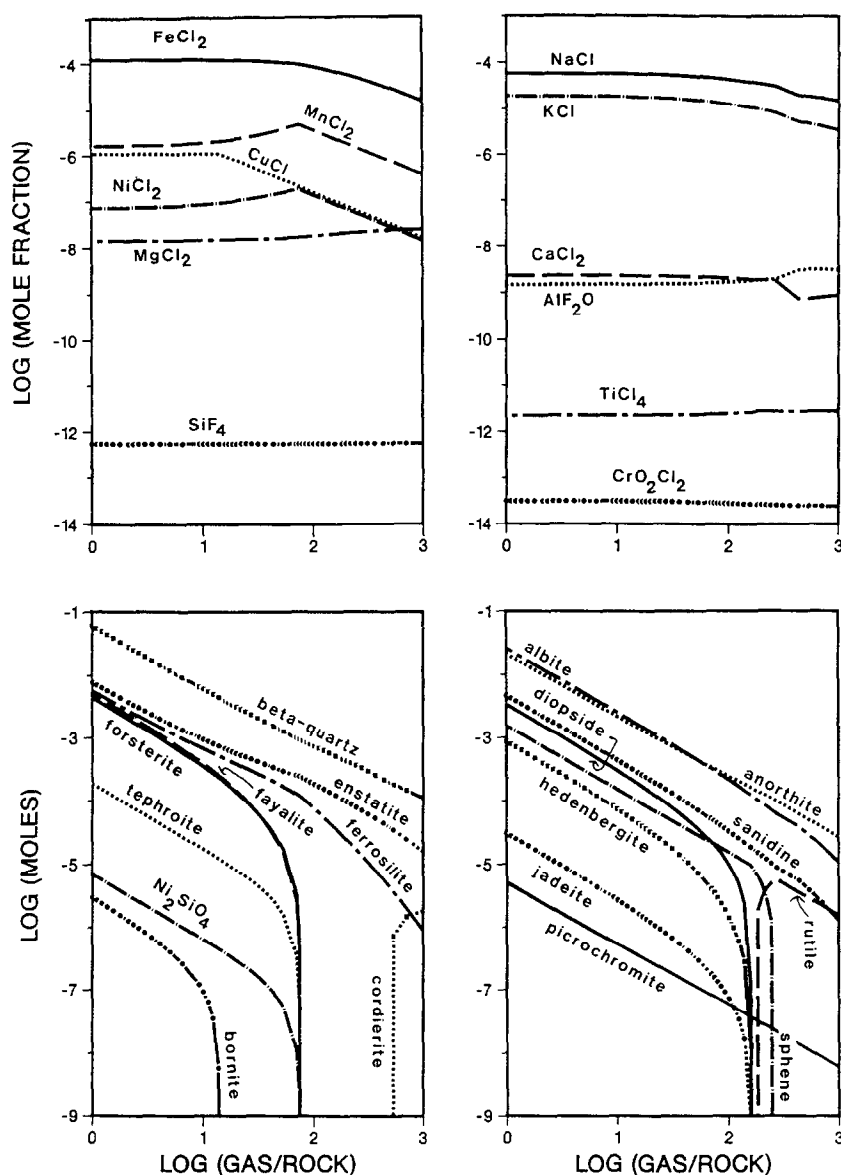
FIG. 6. Calculated heterogeneous equilibrium distribution of gas (top) and mineral (bottom) species for titrating numerically the Augustine andesite into the dome-3 volcanic gas at 870°C and 1 atmosphere pressure. Fugacities of the major species (H_2O, HCl, SO_2, CO_2, H_2S, H_2, S_2, HF, CO, HBr) were fixed by the dome-3 composition (Table 1), but the concentrations of trace components (Fe, Na, K, Mn, Cu, Ni, Mg, Ca, Al, Ti, Si, and Cr) and the equilibrium assemblage of minerals were calculated (by GASWORKS) at gas/rock ratios varying from 1000 to 1.0. Solid solutions of specific minerals are described in the text. The gas species shown are the most abundant ones containing their respective trace elements.

fraction of $CaCl_2$ is relatively constant and is controlled by the assemblage beta-quartz, diopside, and orthoenstatite. The concentration of $CuCl$ increases until it is buffered by bornite, orthoferrosilite, and quartz at LG/R ratios below 1.1. The abundances of SiF_4 and CrO_2Cl_2 are essentially constant at G/R ratios from 1000 to 0.01; SiF_4 is buffered by quartz and the abundance of CrO_2Cl_2 is fixed by the assemblage picro-chromite, orthoenstatite, and beta-quartz.

In contrast to other elements, Mg and Al are more volatile at high G/R ratios than at lower G/R ratios. The volatility of $MgCl_2$ rises with the G/R ratio as the mole fraction of orthoenstatite in orthopyroxene increases. Al, which is vol-

atilized from anorthite, increases at high G/R ratios in response to the simultaneous decrease in $CaCl_2$.

Gas-Andesite Titrations at 870–1050°C and 1 Atmosphere

Since the magmatic temperature at Augustine may be as high as 1050°C (JOHNSTON, 1978), the above calculations were repeated from 870 to 1050°C. We used a fixed G/R ratio of 1 over this temperature range, which generally preserves the same final mineral assemblage, except that beta-tridymite replaces beta-quartz at 871°C and bornite evaporates into the gas between 930 and 960°C. Fugacities of the

major gases were fixed at each temperature increment; their equilibrium distribution was constrained by the dome-3 mass balance (Table 1) and the assumed fO_2 buffer, 0.07 log units below NNO (SYMONDS, 1990).

The results (Fig. 7) show that higher temperatures cause the solubility of trace elements in the gas to increase as one would expect. The volatilities of Fe, Na, Cu, Mn, Ni, Mg, Ca, Al, Ti, and Cr increase, generally by an order of magnitude, as the temperature rises from 870 to 1050°C. One exception is Si, whose volatility (as SiF_4) decreases with increasing temperature.

Comparison of Calculated vs. Observed Mineral Assemblage

One check on the validity of the numerical simulations is to compare the calculated mineral assemblage with that observed in the Augustine andesite. Such comparison is difficult because the calculations assume that the magma is totally crystalline, whereas the erupted pumice fragments have a large percentage of glass, 30–80% in 1976 (JOHNSTON, 1978). Nonetheless, similarity between the computed and observed minerals lends credence to the numerical results.

The final calculated equilibrium assemblage consists of beta-quartz, plagioclase, orthopyroxene, olivine, clinopyroxene, sphene, picrochromite, and bornite. This is in good agreement with the observed mineral assemblages in the 1976 and 1986 Augustine andesite, which consists of plagioclase, augite, orthopyroxene, olivine, Cu-Fe sulfides (chalcopyrite surrounding pyrrhotite), Ti-bearing magnetite, and Cr-rich spinel (JOHNSTON, 1978; HARRIS et al., 1987; Symonds, unpubl. data).

The major differences between the observed and calculated mineral assemblage (at a G/R ratio of 1.0) are that the latter

FIG. 7. Calculated volatilities (at a gas/rock ratio of 1) of the most abundant (for each component) trace gas species for the dome-3 volcanic gas from 870 to 1050°C and 1 atmosphere pressure. The mass balance of the dome-3 major gas composition (Table 1) and the assumed oxygen fugacity trend (.07 units below NNO) were used to fix the fugacities of the major species (H_2O, HCl, SO_2, CO_2, H_2S, H_2, S_2, HF, CO, HBr) as a function of temperature. The equilibrium species of minerals are the same as those at a gas/rock ratio of 1.0 in Fig. 6.

contains beta-quartz and contains sphene instead of Ti-bearing magnetite. Incomplete crystallization of the quartz-normative Augustine lavas explains the absence of late-stage quartz. The absence of Ti-bearing magnetite in the computed assemblage could have resulted from an oversimplified solid solution model for magnetite as natural magnetites contain minor amounts of Mg, Al, and other elements that might enhance their stability.

The general agreement between the calculated and observed mineral assemblages supports the validity of the calculations and the volatilities. Such agreement is evidence for the generally good quality of the thermochemical data and for the existence of many of the computed gas species.

Calculated Volatilities vs. Observed Concentrations

The calculated volatilities for the dome-3 gas composition at 870°C and a G/R ratio of 1 are shown in Table 6. Very similar results (not shown) are also obtained for the dome-2 gas composition. At the current stage of development, potential problems with our gas thermodynamic data lie more in their incompleteness, limiting the number of species we can treat for each element, than in erroneous values. Omission of gas species from the calculations that are present in the actual gas causes an underestimate of volatility. Thus, gas components whose computed volatilities equal or exceed their measured values are more likely to have been volatilized from magma than are those whose computed volatilities are much less than observed concentrations.

Since the calculated volatilities for Fe, Na, K, Mn, Cu, and Ni at 870°C are slightly higher than their analyzed concentrations (Table 6), and even larger volatilities are calculated at higher temperatures (Fig. 7), the calculations indicate that these elements may be volatilized from near-surface magma close to 870°C. Since the volatility of Mg is only 0.4–0.5 log units below the analyzed concentration at 870°C (Table 6) and exceeds the analyzed concentrations above 947°C (Fig. 7), it too may be partly or wholly derived by volatile transport. This does not apply for Al, Ca, Cr, Si, and Ti as they are several orders of magnitude more abundant than predicted. The anomalous concentrations of these elements could mean that they are derived from some other source, or that the computed values are incorrect owing to missing species.

The above calculations suggest that the amounts of Na, K, Fe, Cu, Ni, Mn, and some or all of the Mg in the Augustine dome gases can be explained by volatilization from shallow magma near 870°C. By using the final equilibrium mineral assemblage (at a G/R ratio of 1) along with the most stable gas species, we can speculate on volatilization reactions for each metal in the gas. On this basis, we propose the following volatilization reactions:

$$2NaAlSi_3O_8 + 2HCl + CaMgSi_2O_6$$
$$\text{(albite)} \qquad\qquad \text{(diopside)}$$

$$= MgSiO_3 \qquad + H_2O + CaAl_2Si_2O_8$$
$$\text{(orthoenstatite)} \qquad\qquad \text{(anorthite)}$$

$$+ 2NaCl + 5SiO_2, \qquad (10)$$
$$\text{(beta-quartz)}$$

Table 6.   Calculated volatilities for trace elements in the dome-3
and moat-4 volcanic gases using gas/rock titrations.   All
trace element concentrations data in total mole fraction.

	Dome-3		Moat-4		
	Calculated	Observed	Calculated	Calculated	Observed
$T^\circ C$	870	870	642	642	642
fO_2	-12.59	-12.59	-18.0	-10.0	?
G/R	1.0	?	1.0	1.0	?
Fe	1.3×10^{-4}	1.6×10^{-6}	8.5×10^{-7}	9.5×10^{-8}	2.7×10^{-7}
Na	6.9×10^{-5}	1.4×10^{-5}	3.0×10^{-7}	2.5×10^{-7}	7.7×10^{-7}
K	2.0×10^{-5}	8.7×10^{-6}	8.1×10^{-8}	6.8×10^{-8}	3.4×10^{-7}
Mn	1.7×10^{-6}	1.7×10^{-8}	1.8×10^{-8}	1.1×10^{-7}	5.6×10^{-9}
Cu	1.1×10^{-6}	6.9×10^{-8}	1.7×10^{-9}	1.2×10^{-5}	3.3×10^{-7}
Ni	7.6×10^{-8}	2.2×10^{-9}	3.6×10^{-10}	2.1×10^{-9}	$<1.5 \times 10^{-9}$*
Mg	1.5×10^{-8}	4.8×10^{-8}	7.6×10^{-12}	1.3×10^{-11}	9.5×10^{-8}
Al	1.5×10^{-9}	2.7×10^{-7}	2.5×10^{-9}	6.3×10^{-8}	3.6×10^{-7}
Ca	2.3×10^{-9}	4.6×10^{-7}	4.9×10^{-13}	3.3×10^{-13}	2.2×10^{-7}
Ti	2.3×10^{-12}	6.5×10^{-9}	1.8×10^{-12}	8.3×10^{-13}	3.2×10^{-8}
Si	5.8×10^{-13}	8.3×10^{-5}	1.8×10^{-8}	1.8×10^{-8}	3.0×10^{-5}
Cr	3.4×10^{-14}	1.2×10^{-9}	3.9×10^{-19}	6.2×10^{-15}	$<3.4 \times 10^{-10}$*

* = Maximum concentration based on detection limit.
G/R = Gas/rock ratio used in the calculations.

$$2KAlSi_3O_8 + 2HCl + CaMgSi_2O_6$$
(sanidine)   (diopside)

$$= MgSiO_3 \quad + H_2O + CaAl_2Si_2O_8$$
(orthoenstatite)   (anorthite)

$$+ 2KCl + \quad 5SiO_2, \quad (11)$$
(beta-quartz)

$$Cu_5FeS_4 + 7HCl + 1/2H_2 = 5CuCl + FeCl_2 + 4H_2S,$$
(bornite)

$$(12)$$

$$MgSiO_3 \quad + 2HCl$$
(orthoenstatite)

$$= MgCl_2 + H_2O + \quad SiO_2, \quad (13)$$
(beta-quartz)

$$FeSiO_3 \quad + 2HCl$$
(orthoferrosilite)

$$= FeCl_2 + H_2O + \quad SiO_2, \quad (14)$$
(beta-quartz)

$$Mn_2SiO_4 + 4HCl$$
(tephroite)

$$= 2MnCl_2 + 2H_2O + \quad SiO_2, \quad (15)$$
(beta-quartz)

$$Ni_2SiO_4(s) + 4HCl$$

$$= 2NiCl_2 + 2H_2O + \quad SiO_2. \quad (16)$$
(beta-quartz)

To explain the large concentrations of Al, Ca, and Ti in the dome condensates, we favor an erosive source (see earlier discussion). Mg may also have a significant erosive component. Contamination of magmatic gases by eroded rock particles is consistent with the near-unity Mg enrichment factors for Ba, Al, and Ti in the dome condensates (SYMONDS et al., 1990). An enrichment factor of 7 for Ca is permissive of a volatile source (SYMONDS et al., 1990), but does not preclude contamination from rock particles. We favor rock erosion as the source for Ca because of its low volatility.

The origins of Cr and Si are enigmatic; enrichment factors of 50 and 151, respectively, are not consistent with a wall-rock origin (SYMONDS et al., 1990), but the volatilities are also too small to account for the abundances of these elements. In addition, spheres of cristobalite (SiO_2) are ubiquitous over the entire temperature range (870–400°C) of the silica tube used to collect sublimates from the dome vent, and Cr has large Al enrichment factors (14–335) in the same set of samples, suggesting a volatile source (Symonds and Finnegan, unpubl. data). We have considered two explanations: (1) contamination of Si from the silica tubes used to collect sublimates and condensates and (2) the computed volatilities for Si and Cr are too low because of inconsistent or incomplete thermochemical data.

To test the hypothesis that Si is derived from silica-tube contamination, we calculated the volatility of Si from 870 to 100°C assuming it was in equilibrium with amorphous SiO_2 and the dome-3 gas (without trace components, except Si and Br), and that the gas cooled as a closed system. Figure 8 shows that the volatility of SiF_4 (the most abundant gaseous species of Si) increases by nine orders of magnitude from 870 to 100°C and is large enough to explain the observed Si concentration (Table 6) below 150°C; volatilization of the
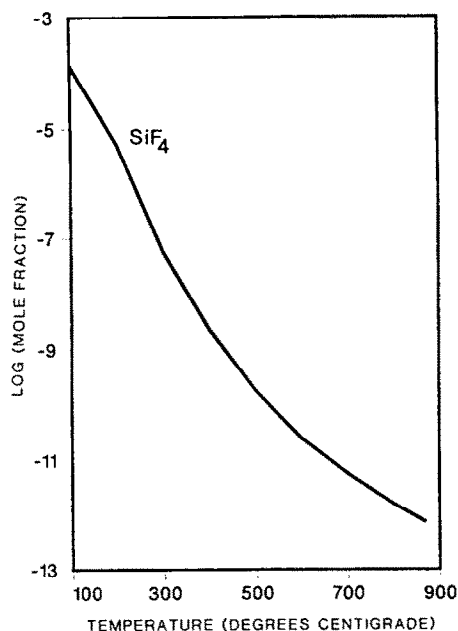
FIG. 8. Calculated volatility of SiF$_4$, the most abundant gas species of Si, in equilibrium with the dome-3 gas composition and amorphous SiO$_2$ as a function of temperature from 870–100°C and 1 atmosphere pressure. Calculations assume closed-system cooling; the oxygen fugacity is determined by the mass balance of the dome-3 sample and thermochemical data. Note how the volatility of SiF$_4$ increases with decreasing temperature.

silica sampling tube can account for the Si contents in the gas condensates. Thus, Si can be volatilized from the silica tube by the reaction:

$$SiO_2 + 4HF = SiF_4 + 2H_2O. \quad (17)$$
(amorphous)
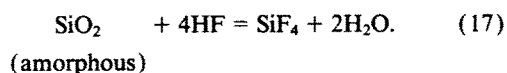
After equilibrating with silica, the gas is supersaturated with respect to beta-quartz, alpha-quartz, and cristobalite (SYMONDS, 1990). The resulting gas remains supersaturated with the SiO$_2$ polymorphs if it does not cool more than 30 to 40°C without re-equilibrating with the silica tube (SYMONDS, 1990). Therefore, redeposition of the volatilized SiF$_4$ can also explain the origin of the cristobalite spheres along the length of the silica tube (1) if metastable cristobalite forms in lieu of alpha- and beta-quartz because of kinetic or solid solution (e.g., substitution of Al^{+3} for Si^{+4}) effects; (2) if the gas does not cool too much before cristobalite is precipitated; and (3) if the gas keeps volatilizing the silica tube as it cools (SYMONDS, 1990). Thus, precipitation of cristobalite may occur via the reaction:

$$SiF_4 + 2H_2O \rightarrow SiO_2 + 4HF, \quad (18)$$
(cristobalite)
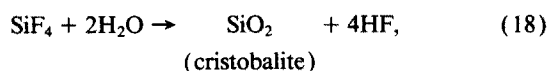
where the arrow indicates that the gas is supersaturated with respect to cristobalite after equilibration with the silica tube.

It is also possible that the calculated volatilities for Si and Cr are too low because the model is missing key gas species for these elements. Our model considers forty-eight species of Si and Cr including chloride, fluoride, bromide, oxyhalide, sulfide, oxide, hydride, elemental, and other gas species (Table

2), but due to the lack of thermochemical data does not include oxyacid species for either element. If the program lacks the dominant gas species of Si and Cr, we suggest that H$_4$SiO$_4$ and H$_2$CrO$_4$ could be those key "missing" species for Si and Cr because (1) H$_2$O is the dominant gas at Augustine so oxyacids are plausible "missing" species; (2) quartz is highly soluble in supercritical H$_2$O as SiO$_2 \cdot$ nH$_2$O (HOLLAND and MALININ, 1979); (3) Cr^{6+} has a high ionic potential and an intermediate electronegativity, suggesting it is transported as an oxyacid in hydrothermal solutions (CRERAR et al., 1985); and (4) oxyacids (e.g., H$_3$BO$_3$, H$_2$MoO$_4$, H$_2$WO$_4$, HReO$_4$) are apparently the dominant species of other elements in high-temperature volcanic gases (SYMONDS et al., 1987; QUISEFIT et al., 1989; BERNARD et al., 1990).

Thus, most of the Si may come from contamination from the silica sampling tube or it may be volatilized entirely from magma as H$_4$SiO$_4$ or some other "missing" species. The Cr enigma can be explained if Cr was volatilized from magma and our model does not include the dominant Cr gas species (e.g., H$_2$CrO$_4$). Spectroscopic studies on volcanic gases should be done to identify possible missing species.

Gas-Andesite Titrations for the Oxidized Moat Vents

The moat gases are cooler, more oxidized, and contain less S and HCl than the dome gases (SYMONDS et al., 1990). They also have higher concentrations of the Type 2 elements and lower concentrations of the Type 1 elements than the dome gases (Fig. 1). To understand the chemical processes that control the latter, it is necessary to repeat the volatility calculations for the moat vents.

For the moat titrations, we used the moat-4 gas composition and a temperature of 642°C, which was measured at the vent. The calculations were done over a range of fO$_2$ conditions because the exact fO$_2$ is unknown. We started the calculations by fixing fO$_2$ at 10^{-18}; fugacities of H$_2$O, HCl, SO$_2$, CO$_2$, H$_2$S, H$_2$, S$_2$, HF, CO, and HBr were also set using the moat-4 mass balance and fO$_2$. We then added increments of andesite (Table 5) until the G/R ratio reached 1; a G/R ratio of 1 was used to compare with the calculations for the dome-3 gas. Successive calculations were done by varying fO$_2$, but using the same amount of titrated rock. Fugacities of H$_2$O, SO$_2$, CO$_2$, H$_2$S, H$_2$, S$_2$, and CO changed appropriately for each fO$_2$.

When fO$_2$ is near NNO, the stable mineral assemblage (Fig. 9) is similar to that observed for the dome-3 gas composition at low G/R ratios (Fig. 6), except that ilmenite (FeTiO$_3$) is present instead of sphene. As fO$_2$ increases, however, the mineral assemblage changes:

1) magnetite-ulvöspinel starts precipitating at a log fO$_2$ of −17.4;
2) sphene replaces ilmenite at a log fO$_2$ of −17.3;
3) chalcocite (Cu$_2$S) replaces bornite at a log fO$_2$ of −15.9;
4) sphene is replaced by rutile at a log fO$_2$ of −15.2;
5) CuCl(c) replaces chalcocite at a log fO$_2$ of −15.0;
6) magnetite-ulvöspinel is replaced by hematite and rutile at a log fO$_2$ of −13.3;
7) the mole fractions of forsterite and fayalite in olivine decrease, which increases the relative mole fractions of tephroite and Ni$_2$SiO$_4$; and
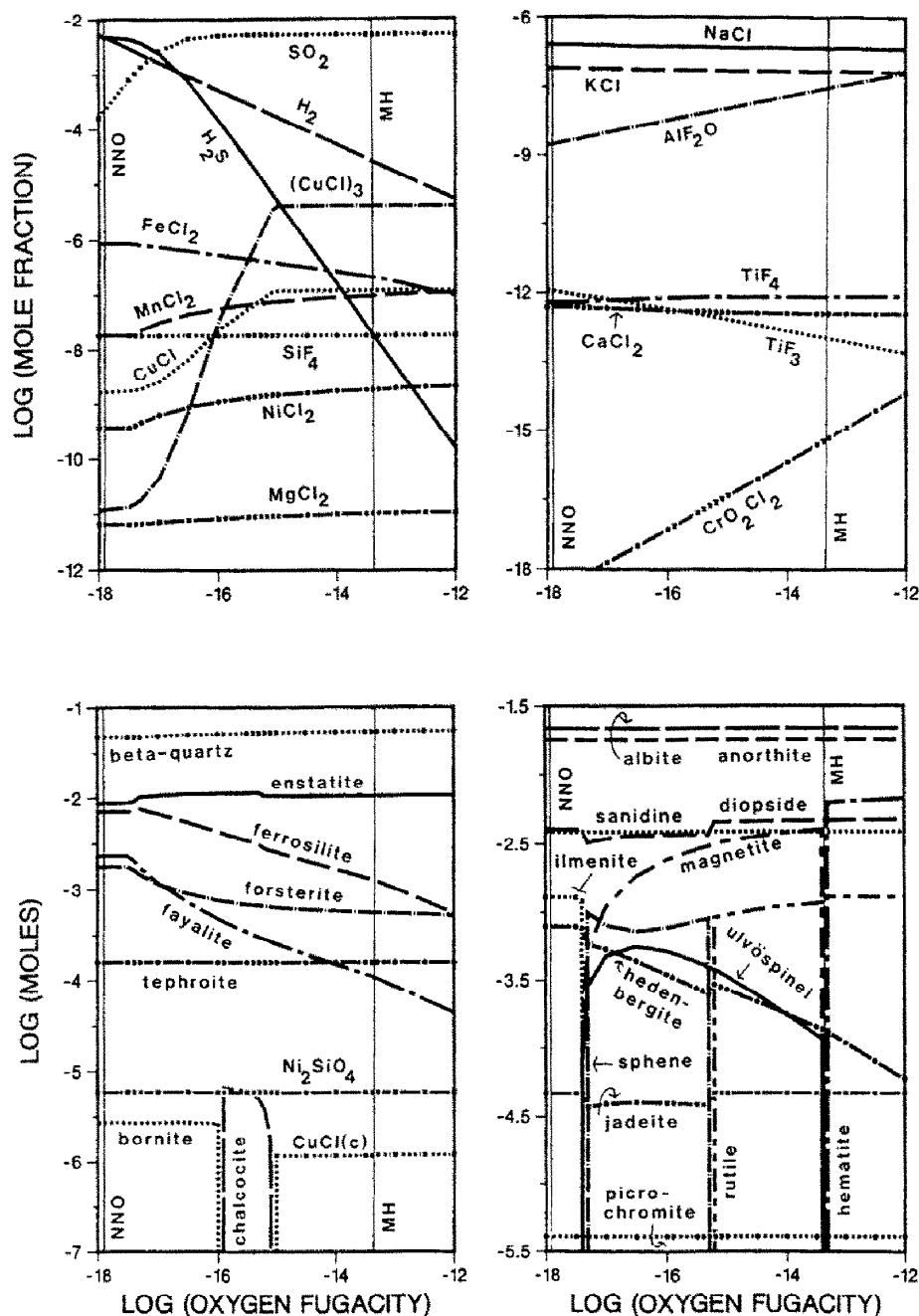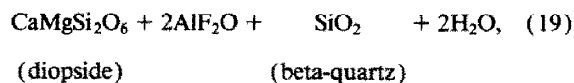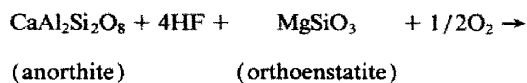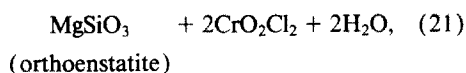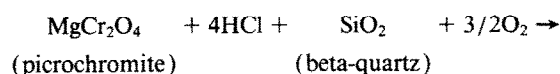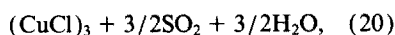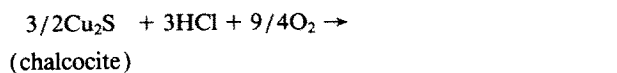
FIG. 9. Calculated heterogeneous equilibrium distribution of gas (top) and mineral (bottom) species after titrating numerically the Augustine andesite into the moat-4 volcanic gas at various oxygen fugacities. Calculations were done at the vent temperature of 642°C, 1 atmosphere pressure and at a gas/rock ratio of 1. The mass balance of the moat-4 gas composition (Table 1) was used to fix the fugacities of the major species (H_2O, HCl, SO_2, CO_2, H_2S, H_2, S_2, HF, CO, HBr) as a function of the oxygen fugacity. Solid solutions between mineral phases are the same as in Fig. 6. The vertical lines represent the positions of the Ni-NiO (NNO) and hematite-magnetite (HM) oxygen buffers at 642°C. Only the most abundant gas species for each component are shown.

8) the mole fraction of hedenbergite in clinopyroxene subsides (Fig. 9).

The calculations show that volatilities of Cu, Mn, Al, Cr, and Ni all increase with fO_2 (Fig. 9). The abundances of AlF_2O, $(CuCl)_3$, and CrO_2Cl_2 increase as O_2 is added because of reactions such as the following:

$$CaAl_2Si_2O_8 + 4HF + \quad MgSiO_3 \quad + 1/2O_2 \rightarrow$$
$$\text{(anorthite)} \qquad\qquad \text{(orthoenstatite)}$$

$$CaMgSi_2O_6 + 2AlF_2O + \quad SiO_2 \quad + 2H_2O, \quad (19)$$
$$\text{(diopside)} \qquad\qquad \text{(beta-quartz)}$$

$$3/2Cu_2S + 3HCl + 9/4O_2 \rightarrow$$
(chalcocite)

$$(CuCl)_3 + 3/2SO_2 + 3/2H_2O, \quad (20)$$

$$MgCr_2O_4 + 4HCl + SiO_2 + 3/2O_2 \rightarrow$$
(picrochromite)   (beta-quartz)

$$MgSiO_3 + 2CrO_2Cl_2 + 2H_2O, \quad (21)$$
(orthoenstatite)

These reactions are written using the dominant gas and mineral species. The arrows indicate that the reactions are driven to the right by oxidation, corresponding to the changes shown graphically in Fig. 9, reading the graphs from left to right. Oxidation drives the production of oxidized gas species (AlF_2O, SO_2, CrO_2Cl_2, H_2O) at the expense of reduced gas species and minerals. The volatilities of Mn and Ni increase under oxidizing conditions because the mole fractions of tephroite and Ni_2SiO_4 in olivine increase.

As discussed above, if the volatility is equal to or greater than the analyzed concentration in the gas condensates, then it is evidence for volatilization of that element. The volatilities of Fe, Cu, and Ni for the moat-4 gases are in best agreement with their analyzed concentrations when fO_2 is between NNO and HM (Table 6; Fig. 9). Under these fO_2 conditions, the moat-4 gases can volatilize enough Fe, Mn, Cu, and Ni to explain the observed concentrations. Since the volatilities of Na and K are only slightly lower than their analyzed concentrations, they too may come mostly from a volatile source. However, volatile transport cannot account for the larger observed concentrations of Al, Mg, Ca, Ti, Si, and Cr in the moat-4 condensates; these discrepancies reflect wall-rock (Al, Mg, Ca, Ti) and silica-tube (Si) contamination in the moat condensates, and possible missing gas species (for Si and Cr) in our model.

Metal volatilities (Table 6) are generally lower for the moat-4 gases than for the dome gases because they are cooler and have less HCl. This explains why the moat-4 gases contain less Fe, Na, K, Mn, and Ni than the dome gases. The calculations also account for the larger concentrations of Cu in the more oxidized, but cooler, moat vents because the volatility of Cu increases with oxidation owing to the destruction of Cu sulfides (bornite, chalcocite), yielding SO_2 gas (Fig. 9).

The above calculations also elucidate why the oxidized moat gases might contain more Mo and Zn than the hotter, more reduced dome gases. In the Augustine lavas, Zn exists in Cr-rich spinel (JOHNSTON, 1978), but may also be incorporated in magnetite; it has not been detected in sulfides (JOHNSTON, 1978; Symonds, unpubl. data). Assuming most of the Zn is in magnetite (spinel is just an accessory phase included in olivine), then larger concentrations of Zn in the moat gases could be explained by high-temperature oxidation of magnetite; as magnetite oxidizes to hematite, $ZnCl_2$ may be volatilized. The sites of Mo in the Augustine lavas are not known. Mo^{+4} (65 pm) has a similar ionic radius (CN = 6) to Ti^{+4} (60.5 pm) and Fe^{+3} (55 pm) (SHANNON, 1976) and may substitute for them in magnetite or other mafic minerals. If Mo occurs as Mo^{+4} in the magma, oxidation could liberate MoO_2Cl_2, which has an oxidation state of +6 for Mo.

## ORIGIN OF NONVOLATILE ELEMENTS

Volatilization from magma or hot wall rock cannot account for the trace amounts of Al, Ca, and Ti in the dome and moat-4 condensates; Mg may also have a nonvolatile source, especially in the moat-4 vent. In addition, low Mg-enrichment factors are evidence that the Augustine condensates contain other nonvolatile elements: (1) Ba and Sr in the dome samples; (2) Ba, Sr, and Mn in the moat samples; (3) Ba, Sr, Mn, and Na in the solfatara samples; and (4) Ba, Sr, Mn, Na, and Fe in the pyroclastic flow samples (SYMONDS et al., 1990). These refractory elements may come from wall-rock erosion (process 2; Fig. 2) as suggested earlier for the high-temperature dome and moat vents; in addition, entrainment of acids that condensed on and dissolved the fumarole walls (process 4; Fig. 2) may be possible in cooler vents. Boiling of water into the gas that has leached the surrounding andesite (process 3; Fig. 2) has been discounted as a viable mechanism for adding refractory elements to the gas (see previous discussion).

Stability of Sulfuric Acid

To see if acid droplets could form on the walls of the Augustine fumaroles and then dissolve them, we tested the stability of sulfuric acid (H_2SO_4) and various hygroscopic derivatives ($H_2SO_4 \cdot H_2O$, $H_2SO_4 \cdot 2H_2O$, $H_2SO_4 \cdot 3H_2O$, $H_2SO_4 \cdot 4H_2O$, $H_2SO_4 \cdot 6.5H_2O$) using the program GAS-WORKS. Sulfuric acid boils at 330°C so we only examined its formation in the low-temperature pyroclastic flow and solfatara fumaroles. We also did not consider the formation of HCl and HF liquids because they are gases at 25°C or above; once a liquid phase (e.g., hygroscopic sulfuric acid, water) forms, however, HCl and HF could dissolve in that solution, decreasing pH.

We tested whether acids could form in the pyroclastic flow and solfatara vents between 330 and 100°C using a gas consisting of 0.9999 moles H_2O, 0.0001 moles total S, and variable amounts of O_2; we used a maximum estimate of total S for these vents (SYMONDS et al., 1990) to optimize the stability of acidic species. We only considered a simplified H-O-S system because complete gas compositions are not available for these vents; adding minor amounts of other components does not affect the results significantly.

The stability of $H_2SO_4 \cdot nH_2O$ liquids increases with decreasing temperature and increasing fO_2; the latter reflects the increasing oxidation state of gaseous sulfur, which goes from -2 (H_2S) to $+4$ (SO_2) to $+6$ (H_2SO_4). However, even under highly oxidizing conditions, sulfuric acid and its hygroscopic forms are undersaturated above 171°C in a gas with 0.01% S. At 171°C, isothermal oxidation (Fig. 10) of such a gas in an initially reduced state (fO_2 below MH) causes $H_2SO_4 \cdot 2H_2O(l)$ to form via the net reaction:

$$H_2S + 2O_2 + 2H_2O \rightarrow H_2SO_4 \cdot 2H_2O(l). \quad (22)$$
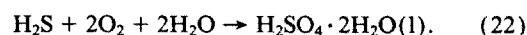
In addition to fO_2, the stability of sulfuric acid and its hygroscopic derivatives depends on the amount of S in the volcanic gas and temperature. To examine the relationship between S content and temperature, we calculated the heterogeneous equilibrium distribution of gas and liquid species
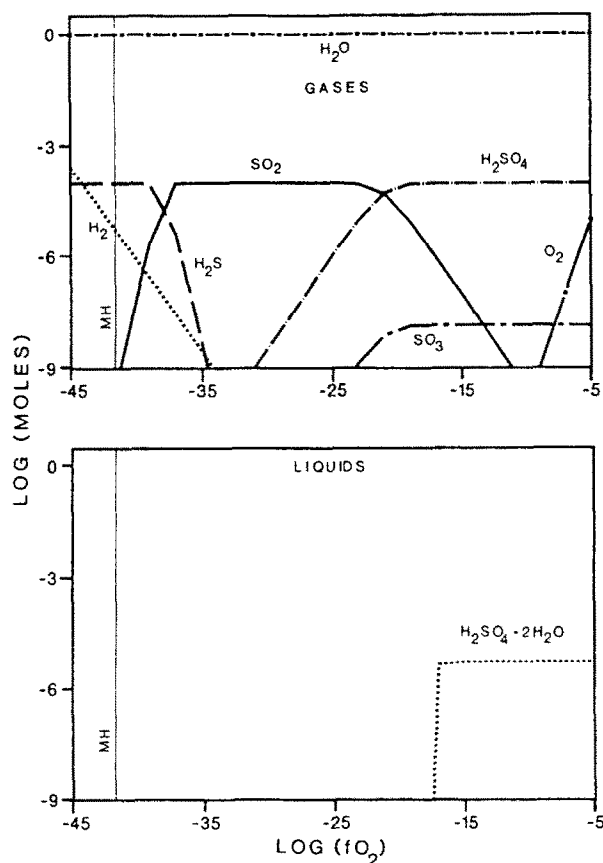
FIG. 10. Calculated heterogeneous equilibrium distribution of gas (top) and acidic liquid (bottom) species in a hypothetical H-O-S gas consisting of 0.9999 moles H_2O, 0.0001 moles total S, and variable amounts of oxygen. Calculations were done at 171°C over a range of fO_2 conditions. For reference the hematite-magnetite (HM) buffer is shown. All data are in log moles.

from 300 to 105°C for five gas compositions: (1) 0.99999 moles H_2O and 0.00001 moles total S, (2) 0.9999 moles H_2O and 0.0001 moles total S, (3) 0.999 moles H_2O and 0.001 moles total S, (4) 0.99 moles H_2O and 0.01 moles total S, and (5) 0.9 moles H_2O and 0.1 moles total S (Fig. 11). In each case, fO_2 was fixed at 10^{-5} to maximize the stability of the acidic liquids.

For each composition, we have plotted the distribution of acidic liquids that form upon cooling (Fig. 11). The results show that the maximum temperature of sulfuric acid deposition is directly proportional to S content; initial deposition temperatures are 261, 221, 199, 171, and 154°C for systems with 0.1, 0.01, 0.001, 0.0001, and 0.00001 moles of S, respectively (Fig. 11). After initial deposition, further cooling causes the liquids to become more hygroscopic; $H_2SO_4 \cdot 2H_2O$ replaces $H_2SO_4 \cdot H_2O$ at 199°C, $H_2SO_4 \cdot 3H_2O$ replaces $H_2SO_4 \cdot 2H_2O$ at 161°C, $H_2SO_4 \cdot 4H_2O$ replaces $H_2SO_4 \cdot 3H_2O$ at 142°C, and $H_2SO_4 \cdot 6.5H_2O$ replaces $H_2SO_4 \cdot 4H_2O$ at 125°C (Fig. 11).

Even in highly oxidized volcanic gases, acidic liquids will not form above 202°C, the lowest temperature vent sampled by SYMONDS et al. (1990), unless the gases have more than 0.1% S, 10 to 1000 times higher than in the solfatara or py-

roclastic flow vents (SYMONDS et al., 1990). Even with 10% S, $H_2SO_4 \cdot H_2O$ will not form unless the temperature is 261°C or below (Fig. 11). Thus, sulfuric acid droplets are not stable in any of the vents sampled by SYMONDS et al. (1990), but could have formed in lower temperature (<202°C) vents in the pyroclastic flow and solfatara fumarole fields. Below 202°C, the sulfuric acid would most certainly be hygroscopic (Fig. 11) and could react with the wall rock.

Condensate-Rock Titrations

If refractory elements do not come from meteoric water that leached andesite and boiled into the gas stream or from acids that condensed on and reacted with the walls of fumaroles, then they may come entirely from wall-rock erosion (process 2; Fig. 2). Numerical titrations using the methods of REED (1982) can be used to decide which elements are derived by wall-rock erosion and to calculate the effective condensate/rock ratios necessary to explain their observed concentrations. For each analysis of condensate (SYMONDS et al., 1990), we titrated Augustine andesite (Table 5) into a hypothetical solution, whose anion concentration matched the respective condensate samples. (Possible variations in the compositions of eroded particles were neglected for this study.) The pH of each hypothetical solution was computed by determining the moles of H^+ (M^t_{H+}; REED and SPYCHER, 1984) necessary for charge balance. All titrations were done at 25°C using an atmospheric oxygen buffer (for redox equilibria). Calculations were done using the program CHILLER (REED, 1982), a heterogeneous equilibrium thermodynamics computer program involving minerals, gases, and an aqueous phase.

To estimate the andesite contribution in each sample, andesite was titrated into each condensate composition until the concentration of Mg in the resulting solution matched that of the analyzed condensate. Magnesium was used for reference because it has a low volatility (Table 6) and its concentration was determined in all the Augustine condensates (SYMONDS et al., 1990); similar results were obtained using Al.

Since the Augustine condensates contain, at most, a few ppm of the major rock-forming elements (e.g., Al), only a small amount of rock-particle contamination is necessary to explain their concentrations. At such high water/rock ratios, no minerals were calculated to saturate with any of these solutions.

Table 7 shows the results of such calculations for the PF-2, solf-3, moat-4A, and dome-1A condensate samples. For refractory elements, the results compare favorably with the analyzed concentrations and suggest that rock-particle erosion is the origin of (1) Mg, Mn, Ba, Fe, Ca, Si, Al, Sr, Na, and possibly K in the PF-2 sample; (2) Mg, Al, Ca, Na, Mn, Ba, Sr, and possibly K in the solf-3 sample; (3) Al, Ca, Mg, Mn, Ba, and Sr in the moat-4A sample; and (4) Al, Mg, Ba, and Sr in the dome-1A sample. Many of these elements also have low volatilities in the moat-4 and dome gases (Table 6; Figs. 6–7, 9), confirming an erosive source. However, since the volatilities can account for the observed concentrations of Mn in the moat-4 gases and some or all of the Mg in the dome gases, they may have significant volatile components.
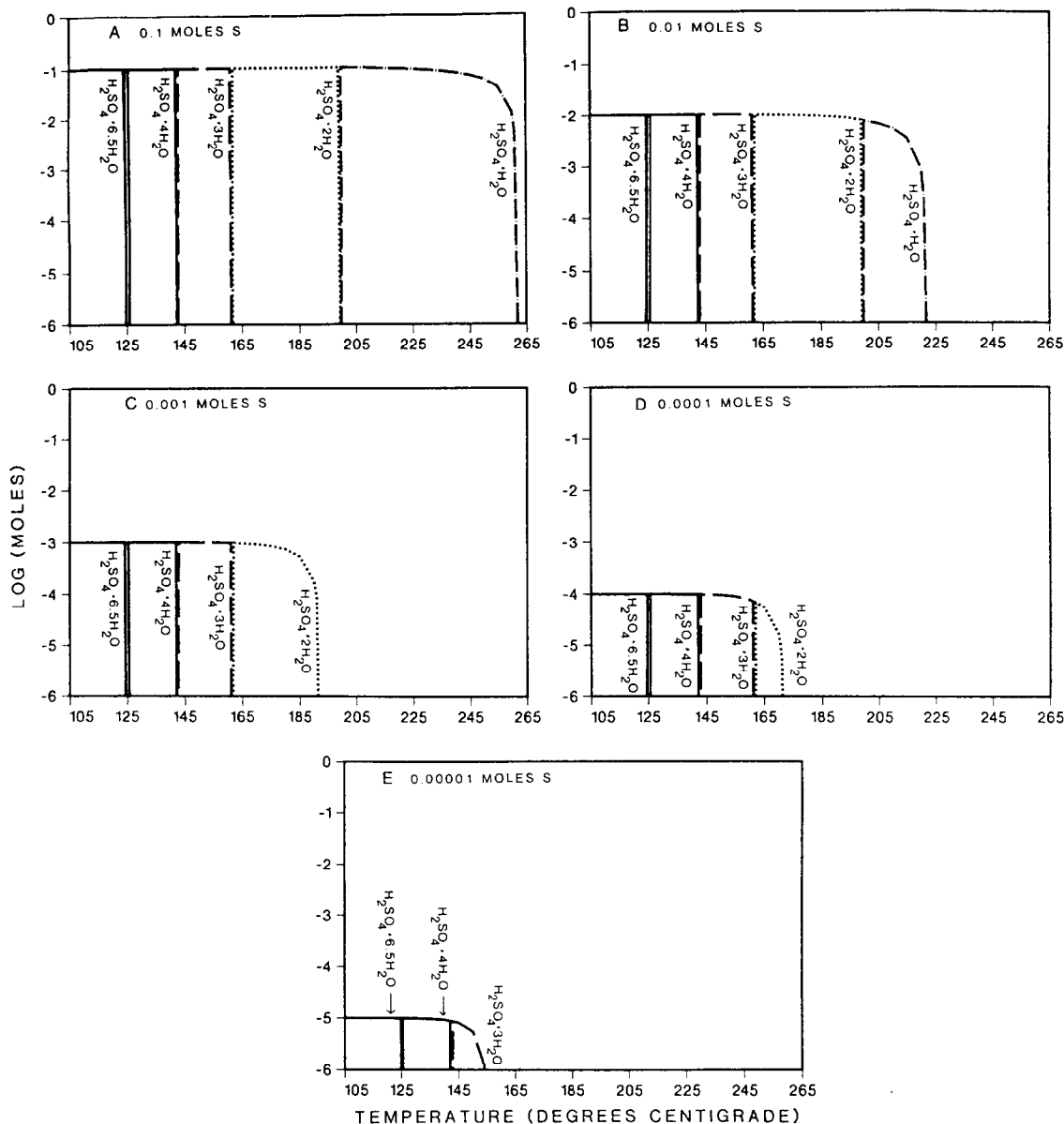
FIG. 11. Calculated distribution of sulfuric acid liquids in five theoretical H-O-S gas compositions: (a) 0.90 moles H_2O and 0.10 moles total S; (b) 0.99 moles H_2O and 0.01 moles total S; (c) 0.999 moles H_2O and 0.001 moles total S; (d) 0.9999 moles H_2O and 0.0001 moles total S; and (e) 0.99999 moles H_2O and 0.00001 moles total S. In each case, fO_2 was fixed at 10^{-5}. All data are in log moles.

Finally, the fact that the above calculations cannot account for observed concentrations of Si in the dome, moat, and solfatara condensates suggests that Si came from volatile transport or silica-tube contamination in these samples.

The water/rock ratios necessary to explain the observed amounts of Mg in each sample are an approximate way to compare the degree of rock interaction in each condensate sample. Figure 12 shows that the water/rock ratio required to explain the observed amount of Mg in each condensate sample is between 10^4 and 10^6. Clearly, only a very small amount of particle erosion is needed to explain the concentrations of Mg in any of the samples.

The amount of rock particle contamination shows no correlation with temperature (Fig. 12); instead, it varies with fumarole type: the pyroclastic flow condensates are most contaminated, the moat condensates are second-most contaminated, and the solfatara and dome samples are the least contaminated. The pyroclastic flow condensates have had the greatest amount of wall-rock contamination because the friable, ashy walls of those vents are much easier to erode than lava, the dominant type of wall rock in the summit fumaroles. Similarly, the moat condensates have a significant erosive component because the moat lava (1976 dome) is covered with tephra. A smaller erosive component also

Table 7. Calculated concentrations of trace elements in selected Augustine gas samples assuming that dissolution of rock particles is the origin of Mg in the respective condensate sample. Augustine andesite was titrated (numerically) into a solution with the same pH and anion concentration as each condensate sample until the calculated Mg concentration matched the observed concentration. For comparison the observed concentrations of trace elements are reported. All data are mole fractions in the total gas.

Sample:	PF-2 Calculated	PF-2 Observed[1]	Solf-2 Calculated	Solf-2 Observed[1]	Moat-4A Calculated	Moat-4A Observed[2]	Dome-1A Calculated	Dome-1A Observed[3]
W/R	29813		126298		153414		306879	
Si	6.3×10^{-6}	2.0×10^{-5}	1.5×10^{-6}	2.4×10^{-5}	1.2×10^{-6}	3.0×10^{-5}	5.1×10^{-7}	8.3×10^{-5}
Al	2.0×10^{-6}	6.5×10^{-6}	4.7×10^{-7}	2.6×10^{-7}	3.8×10^{-7}	3.6×10^{-7}	1.7×10^{-7}	2.7×10^{-7}
Ca	7.3×10^{-7}	1.9×10^{-6}	1.8×10^{-7}	3.5×10^{-7}	1.4×10^{-7}	2.2×10^{-7}	6.2×10^{-8}	4.6×10^{-7}
Fe	4.6×10^{-7}	1.2×10^{-6}	1.1×10^{-7}	2.2×10^{-6}	8.6×10^{-8}	2.7×10^{-7}	3.9×10^{-8}	1.6×10^{-6}
Na	7.3×10^{-7}	2.7×10^{-6}	1.7×10^{-7}	3.0×10^{-7}	1.4×10^{-7}	7.7×10^{-7}	5.9×10^{-8}	1.4×10^{-5}
Mg	5.5×10^{-7}	5.5×10^{-7}	1.3×10^{-7}	1.3×10^{-7}	1.0×10^{-7}	9.5×10^{-8}	4.5×10^{-8}	4.8×10^{-8}
K	1.3×10^{-7}	$<4.7 \times 10^{-7}$	3.0×10^{-8}	$<4.6 \times 10^{-7}$	2.4×10^{-8}	3.4×10^{-7}	1.1×10^{-8}	8.7×10^{-6}
Mn	1.0×10^{-8}	1.2×10^{-8}	2.3×10^{-9}	3.3×10^{-9}	1.9×10^{-9}	5.6×10^{-9}	8.5×10^{-10}	1.7×10^{-8}
Ba	3.9×10^{-9}	7.6×10^{-9}	9.3×10^{-10}	7.9×10^{-10}	7.7×10^{-10}	5.8×10^{-10}	3.2×10^{-10}	2.8×10^{-10}
Sr	2.1×10^{-9}	7.1×10^{-9}	5.0×10^{-10}	6.2×10^{-10}	4.0×10^{-10}	4.0×10^{-10}	1.8×10^{-10}	5.3×10^{-10}
Zn	1.0×10^{-9}	6.5×10^{-7}	2.5×10^{-10}	2.7×10^{-6}	1.9×10^{-10}	5.3×10^{-7}	9.5×10^{-11}	6.4×10^{-7}
Cu	4.3×10^{-10}	3.5×10^{-8}	1.1×10^{-10}	7.7×10^{-7}	8.4×10^{-11}	3.3×10^{-7}	4.9×10^{-11}	6.9×10^{-8}
Pb	2.7×10^{-11}	2.0×10^{-8}	6.1×10^{-12}	1.3×10^{-8}	5.1×10^{-12}	3.7×10^{-8}	2.2×10^{-12}	2.4×10^{-7}
As	4.9×10^{-11}	9.8×10^{-10}	1.2×10^{-11}	1.5×10^{-8}	9.5×10^{-12}	1.3×10^{-7}	4.1×10^{-12}	9.9×10^{-7}
Sb	1.2×10^{-11}	9.1×10^{-10}	3.0×10^{-12}	2.2×10^{-9}	2.9×10^{-12}	1.7×10^{-9}	1.3×10^{-12}	3.8×10^{-8}

[1] Estimated concentration in the gas assuming the condensate sample is the total gas.
[2] Average concentration in the moat-4 gas (Table 1) using the moat-4A and moat-4B condensates.
[3] Average concentration in the dome-3 gas (Table 1) using the dome-1A and dome-1B condensates.
W/R is the water/rock ratio used for the calculations.

FIG. 12. Calculated water/rock ratios that would be necessary to explain the observed Mg concentration in each condensate sample by wall-rock leaching. Note that there is a wide variation in the degree of wall-rock interaction in the various fumaroles and that the pyroclastic flow fumaroles have the highest degree of wall-rock interaction (low water/rock ratio).

explains why the dome condensates have lower geometric mean concentrations of Al, Mg, Ti, Zr, and Ba than the moat samples (Fig. 1).

CONCLUSIONS

Many trace elements in the high-temperature, HCl-rich gases escaping from a fumarole on the 1986 Augustine dome are volatilized directly from near-870°C andesitic magma as chloride (NaCl, KCl, $FeCl_2$, $ZnCl_2$, $PbCl_2$, CuCl, $SbCl_3$, LiCl, $MnCl_2$, $NiCl_2$, BiCl, $SrCl_2$), oxychloride (MoO_2Cl_2), sulfide (AsS), and elemental (Cd) gas species. This study does not support previous suggestions (GEMMELL, 1987) that metals are transported as bromides in volcanic gases. The gases escaping from the moat fumaroles (remains of the 1976 dome) have volatilized less Fe, Na, K, Mn, and Ni because they are 200–400°C cooler than the dome gases. However, the moat gases are also more oxidized than the dome gases, which explains why Cu, and possibly Zn and Mo should be more volatile in these vents. Temperature, HCl fugacity, and oxygen fugacity are extremely important variables in governing the mobility of metals in the Augustine fumaroles.

Some elements are not volatilized from magma; instead, they come from eroded rock particles that subsequently dissolved in the condensates. Elements coming from particle erosion include Al, Ca, Sr, Ba, Ti, V, and possibly Mg and Sr in the dome and moat vents, but also Mn, Na, and possibly K in the solfatara vents; and Mn, Na, Fe, Si, and possibly K in the pyroclastic flow fumaroles. Only a small amount of wall-rock erosion is necessary to explain the observed concentrations of these nonvolatile elements in the Augustine condensates. Erosion is more prevalent in the fumaroles on the 1986 pyroclastic flows because they escape through unconsolidated ash and pumice rather than lava.

Previous studies have shown that the abundances of trace elements in volcanic gas condensates are highly variable, whether the samples are collected at several volcanoes in the same volcanic arc, different fumaroles on one volcano,

or at a single fumarole at different times (STOIBER and ROSE, 1970; GEMMELL, 1987; SYMONDS et al., 1987; SYMONDS et al., 1990). This study suggests that these differences in trace element concentrations are due to large variations in volatilities and the extent of wall-rock erosion. Volatilities are affected by changes in temperature, pressure, the major gas composition, and the composition and degassing state of the magma. The effect of rock-particle contamination depends on the physical nature of the fumarole walls (lava or unconsolidated ash), the gas velocity, and the composition of the wall rock.

The methods used in this paper provide a direct way to use data on volcanic gases to predict the vapor pressures of the major and trace gas species emanating from degassing magma. The validity of these results depends on four factors:

1) whether the gases actually escaped from magma or came from another source;

2) the quality of the gas and condensate data used in modeling;

3) the applicability of the equilibrium assumption; and

4) the quality and quantity of the thermochemical data used in the model.

All four can be evaluated directly by combining studies of volcanic gases and condensates with thermochemical modeling. In contrast to laboratory studies of melt-vapor equilibria (e.g., HAMPTON and BAILEY, 1985; ZBINDEN and STEBBINS, 1988), this method of studying the volatiles released from magmas does not involve any simplifying assumptions regarding the composition of the magma or the carrier gas.

Volcanoes are one source of natural gas emissions to the atmosphere. In order to understand the impact of anthropogenic air pollution on the environment, it is important to understand the magnitude of natural sources of these pollutants. In this paper, we have attempted to constrain the fluxes of major and trace gas species using their equilibrium distribution at high temperature. Future studies should estimate fluxes of these species from other volcanoes and account for particulate and gaseous species that form when volcanic gases mix with the atmosphere.

Our modeling is consistent with the idea that many trace elements in the Augustine gases were volatilized from magma; but its success does not preclude the possibility that a significant quantity of H_2O, HCl, and metals may come from late-stage boiling of seawater or a seawater brine directly into the gas phase. In light of the seawater component for H_2O in Augustine's fumarolic condensates (SYMONDS et al., 1990), future studies should investigate where the seawater enters the magmatic-hydrothermal systems and its possible contribution to the high-temperature fumarolic gases. Such work will shed light on Augustine's eruption mechanisms, the possibility of subsurface brines, and the possible genesis of ore deposits in magmatic-seawater systems.

computer programs. This theoretical study was based on field studies which benefited from generous logistical support by Thomas Miller, John Davies, Juergen Kienle, John Power, Elizabeth Yount, the USGS, and the Alaskan Volcano Observatory.

Editorial handling: G. Faure

REFERENCES

ANDERSON A. T. (1975) Some basaltic and andesite gases. *Rev. Geophys. Space. Phys.* **13**, 37–55.

BERNARD A., SYMONDS R. B., and ROSE W. I., JR. (1990) Volatile transport and deposition of Mo, W and Re in high temperature magmatic fluids. *Appl. Geochem.* **5**, 317–326.

BUAT-MÉNARD P. and ARNOLD M. (1978) The heavy metal chemistry of atmospheric particulate matter emitted by Mount Etna Volcano. *Geophys. Res. Let.* **4**, 245–248.

CASADEVALL T., ROSE W., GERLACH T., GREENLAND L. P., EWERT J., WUNDERMAN R., and SYMONDS R. (1983) Gas emissions and the eruptions of Mount St. Helens through 1982. *Science* **221**, 1383–1385.

CRERAR D., WOOD S., and BRANTLEY S. (1985) Chemical controls on solubility of ore-forming minerals in hydrothermal solutions. *Canadian Mineral.* **23**, 333–352.

DEVINE J. D., SIGURDSSON H., DAVIS A. N., and SELF S. (1984) Estimates of sulfur and chlorine yield to the atmosphere from volcanic eruptions and potential climatic effects. *J. Geophys. Res.* **89**, 6309–6325.

GEMMELL J. B. (1987) Geochemistry of metallic trace elements in fumarolic condensates from Nicaraguan and Costa Rican volcanoes. *J. Volcanol. Geotherm. Res.* **33**, 161–181.

GERLACH T. M. (1980a) Evaluation of volcanic gas analyses from Kilauea Volcano. *J. Volcanol. Geotherm. Res.* **7**, 295–317.

GERLACH T. M. (1980b) Investigations of volcanic gas analyses and magma outgassing from Earta'Ale lava lake, Afar, Ethiopia. *J. Volcanol. Geotherm. Res.* **7**, 414–441.

GERLACH T. M. (1989) Greenhouse forcing by carbon dioxide degassing of basalt: Eruptive vs. noneruptive mechanisms (abstr.). *Geol. Soc. Amer. Abstr. Progr.* **21**, A13.

GERLACH T. and CASADEVALL T. (1986a) Evaluation of gas data from high-temperature fumaroles at Mount St. Helens, 1980–1982. *J. Volcanol. Geotherm. Res.* **28**, 107–140.

GERLACH T. and CASADEVALL T. (1986b) Fumarole emissions at Mount St. Helens Volcano, June 1980 to October, 1981: Degassing of a magma-hydrothermal system. *J. Volcanol. Geotherm. Res.* **28**, 141–160.

GERLACH T. M. and NORDLIE B. E. (1975) The C-O-H-S gaseous system, Part II: Temperature, atomic composition, and molecular equilibria in volcanic gases. *Amer. J. Sci.* **275**, 377–394.

GILL J. B. (1981) *Orogenic Andesites and Plate Tectonics.* Springer-Verlag.

GREENLAND L. P., ROSE W. I., and STOKES J. B. (1985) An estimate of gas emissions and magmatic gas content from Kilauea Volcano. *Geochim. Cosmochim. Acta* **49**, 125–129.

HAMPTON C. M. and BAILEY D. K. (1985) Sublimates obtained during fusion of volcanic glasses. *J. Volcanol. Geotherm. Res.* **25**, 145–155.

HARRIS G. W., SWANSON S. E., and NYE C. J. (1987) Comparative petrology and petrography of the 1976 and 1986 ejecta of Augustine Volcano, Alaska (abstr.). *Geol. Soc. Amer. Abstr. Progr.* **19**, 387.

HOLLAND H. D. and MALININ S. D. (1979) The solubility and occurrence of non-ore minerals. In *Geochemistry of Hydrothermal Ore Deposits* (ed. H. L. BARNES), pp. 461–508. J. Wiley & Sons.

JAESCHKE W., BERRESHEIM H., and GEORGII H. (1982) Sulfur emissions from Mt. Etna. *J. Geophys. Res.* **87**, 7253–7261.

JAGGER T. A. (1940) Magmatic gases. *Amer. J. Sci.* **238**, 313–353.

JOHNSTON D. (1978) Volatiles, magma mixing and explosive mechanism of Augustine Volcano, Alaska. Ph.D. dissertation, Univ. of Washington.

JOHNSTON D. (1980) Volcanic contribution of chlorine to the stratosphere: More significant to ozone than previously estimated? *Science* **209**, 491–492.

KODOSKY L. and KESKINEN M. (1990) Fumarole distribution, mor-

phology, and encrustation mineralogy associated with the 1986 eruptive deposits of Mount St. Augustine, Alaska. *Bull. Volcanol.* **52**, 175–185.

KODOSKY L., MOTYKA R. J., and SYMONDS R. B. (1991) Fumarolic emissions from Mt. St. Augustine, Alaska, 1979–1984: Degassing trends, volatile sources, and their possible role in eruptive style. *Bull. Volcanol.* **53**, 381–394.

LE GUERN F. (1988) Ecoulements gazeux réactifs à hautes températures, mesures et modélisation. Ph.D. dissertation, Univ. Paris.

LEPEL E., STEFANSSON K., and ZOLLER W. (1978) The enrichment of volatile elements in the atmosphere by volcanic activity: Augustine Volcano 1976. *J. Geophys. Res.* **83**, 6213–6220.

NAUGHTON J. J., LEWIS V. A., HAMMOND D., and NISHIMOTO D. (1974) The chemistry of sublimates collected directly from lava fountains at Kilauea Volcano, Hawaii. *Geochim. Cosmochim. Acta* **38**, 1679–1690.

PATTERSON C. C. and SETTLE D. M. (1987) Magnitude of lead flux to the atmosphere from volcanoes. *Geochim. Cosmochim. Acta* **51**, 675–681.

PHELAN J. M., FINNEGAN D. L., BALLANTINE D. S., ZOLLER, W. H., HART M. A., and MOYERS J. L. (1982) Airborne aerosol measurements in the quiescent plume at Mount St. Helens: September, 1980. *Geophys. Res. Lett.* **9**, 1093–1096.

QUISEFIT J. P., BERGAMETTI G., TEDESCO D., PINART J., and COLIN J. L. (1988) Origin of particulate potassium in Mt Etna emissions before and during the 1983 eruption. *J. Volcanol. Geotherm. Res.* **35**, 111–119.

QUISEFIT J. P., TOUTAIN J. P., BERGAMETTI G., JAVOY M., CHEYNET B., and PERSON A. (1989) Evolution versus cooling of gaseous volcanic emissions from Momotombo Volcano, Nicaragua: Thermochemical model and observations. *Geochim. Cosmochim. Acta* **53**, 2591–2608.

REED M. H. (1982) Calculation of multicomponent chemical equilibria and reaction processes in systems involving minerals, gases and an aqueous phase. *Geochim. Cosmochim. Acta* **46**, 513–528.

REED M. H. and SPYCHER N. (1984) Calculation of pH and mineral equilibria in hydrothermal waters with applications to geothermometry and studies of boiling and dilution. *Geochim. Cosmochim. Acta* **48**, 1479–1492.

REED M. H. and SYMONDS R. B. (1992) Calculation of multicomponent chemical equilibria in gas-solid-liquid systems, Part I: Calculation methods. *Amer. J. Sci.* (submitted).

ROSE W. I., CHUAN R. L., and WOODS D. C. (1982) Small particles in plumes of Mount St. Helens. *J. Geophys. Res.* **87**, 4956–4962.

ROSE W. I., CHUAN R. L., GIGGENBACH W. F., KYLE P. R., and SYMONDS R. B. (1986) Rates of sulfur dioxide and particle emissions from White Island volcano, New Zealand, and an estimate of the total fluxes of major gaseous species. *Bull. Volcanol.* **48**, 181–188.

ROSE W. I., HEIKEN G., WOHLETZ K., EPPLER D., BARR S., MILLER T., CHUAN R. L., and SYMONDS R. B. (1988) Direct rate measurements of plumes at Augustine Volcano: A problem of scaling and uncontrolled variables. *J. Geophys. Res.* **93**, 4485–4499.

SHANNON R. D. (1976) Revised effective ionic radii and systematic studies of interatomic distances in halides and chalcogenides. *Acta Cryst.* **A32**, 751–767.

SPYCHER N. F. and REED M. H. (1989) Evolution of a Broadlands-type epithermal ore fluid along alternative P-T paths: Implications for the transport and deposition of base, precious, and volatile metals. *Econ. Geol.* **84**, 328–359.

STOIBER R. E., and ROSE W. I., JR. (1970) The geochemistry of Central American volcanic gas condensates. *Geol. Soc. Amer. Bull.* **81**, 2891–2911.

SWANSON S. E. and KIENLE J. (1988) The 1986 eruption of Mount St. Augustine: Field test of a hazard evaluation. *J. Geophys. Res.* **93**, 4500–4520.

SYMONDS R. B. (1990) Applications of multicomponent chemical equilibria to volcanic gases at Augustine volcano, volcanic halogen emissions, and volcanological studies of gas-phase transport. Ph.D. dissertation, Michigan Technological University.

SYMONDS R. B. and REED M. H. (1992) Calculation of multicomponent chemical equilibria in gas-solid-liquid systems: Part II. thermochemical data and applications to studies of high-temper-

ature volcanic gases with examples from Mount St. Helens. *Amer. J. Sci.* (submitted).

SYMONDS R. B., ROSE W. I., REED M. H., LICHTE F. E., and FINNEGAN D. L. (1987) Volatilization, transport and sublimation of metallic and non-metallic elements in high temperature gases at Merapi Volcano, Indonesia. *Geochim. Cosmochim. Acta* **51**, 2083–2101.

SYMONDS R. B., ROSE W. I., and REED M. H. (1988) Contribution of Cl- and F-bearing gases to the atmosphere by volcanoes. *Nature* **334**, 415–418.

SYMONDS R. B., ROSE W. I., GERLACH T. M., BRIGGS P. H., and HARMON R. S. (1990) Evaluation of gases, condensates, and SO_2 emissions from Augustine volcano, Alaska: The degassing of a Cl-rich volcanic system. *Bull. Volcanol.* **52**, 355–374.

TOUTAIN J. P., ALOUPOGIANNIS P., DELORME H., PERSON A., BLANC P., and ROBAYE G. (1990) Vapor deposition of trace elements from degassed basaltic lava, Piton de la Fournaise volcano, Reunion Island. *J. Volcanol. Geotherm. Res.* **40**, 257–268.

VAREKAMP J. C. and BUSECK P. R. (1986) Global mercury flux from volcanic and geothermal sources. *Appl. Geochem.* **1**, 65–73.

VAREKAMP J. C., THOMAS E., GERMAINI M., and BUSECK P. R. (1986) Particle geochemistry of volcanic plumes of Etna and Mount St. Helens. *J. Geophys. Res.* **91**, 12,333–12,248.

VIE LE SAGE R. (1983) Chemistry of the volcanic aerosols. In *Forecasting Volcanic Events* (eds. H. TAZIEFF and J. C. SABROUX), pp. 445–474. Elsevier.

ZBINDEN E. A. and STEBBINS J. F. (1988) Measurement of melt-vapor equilibria and transport (abstr.). *Eos* **69**, 1465.